Étude du givrage atmosphérique sur un banc d'essai de grande échelle pour l'industrie éolienne – Atmospheric Icing Study on a Large-Scale Test Bench for Wind Energy Applications

par

© THOMAS ALLARD

Mémoire présenté à l'Université du Québec à Chicoutimi en vue de l'obtention du grade de Maîtrise ès sciences appliquées (M. Sc. A.) en ingénierie

Jury :

Dilip Sarkar, président du jury, Université du Québec à Chicoutimi

Gelareh Momen, directrice de recherche, Université du Québec à Chicoutimi,

Marie-Isabelle Farinas, professeure, Université du Québec à Chicoutimi

Cherif Raef, évaluateur externe, Université du Québec à Rimouski

Éric Villeneuve, codirecteur de recherche, Université du Québec à Rimouski

Derek Harvey, codirecteur de recherche, Université du Québec à Chicoutimi

Québec, Canada

RÉSUMÉ

Le givrage atmosphérique des infrastructures énergétiques est devenu un sujet de recherche grandissant au cours des dernières décennies. Son impact est particulièrement important pour les parcs éoliens opérant en conditions nordiques. Pendant les épisodes de givre, des gouttelettes d'eau surfondue peuvent s'accumuler sous forme de glace sur les pales des éoliennes, modifiant leurs performances aérodynamiques et réduisant l'efficacité de la production d'énergie. Ces accumulations de glace peuvent entraîner des pertes annuelles d'énergie substantielles ainsi que des défis opérationnels accrus pour les exploitants de parcs éoliens. En réponse à cette problématique, d'importants efforts de recherche ont été consacrés à la compréhension des mécanismes de givrage et au développement de stratégies efficaces de protection contre la glace pour les pales d'éoliennes.

Ce présent projet vise à développer une méthodologie expérimentale à grande échelle pour la caractérisation du givrage atmosphérique et des systèmes passifs de protection contre le givre appliqués aux pales d'éoliennes. Compte tenu de la disponibilité limitée de données expérimentales obtenues dans des conditions de givrage réalistes et contrôlées à des échelles représentatives, cette recherche propose un cadre expérimental approfondi permettant de combler l'écart entre les mesures réalisées à petite échelle en laboratoire et les performances observées sur le terrain.

Cette étude est organisée en deux phases principales. La première phase porte sur la finalisation et la calibration d'un banc d'essai à grande échelle à pales rotatives installé dans une chambre climatique. Les principaux paramètres gouvernants les conditions givrantes sont mesurés et caractérisés afin d'assurer une bonne répétabilité et représentativité du terrain. La procédure d'essai d'adhérence de la glace développée repose sur le délestage centrifuge de la glace et sur un appareil dédié à la mesure de la résistance cohésive de la glace. Cet appareil est utilisé conjointement avec le banc d'essai principal afin d'améliorer l'interprétation des événements partiels de détachement de glace observés lors des essais. La fiabilité et la répétabilité de la procédure expérimentale sont évaluées au moyen d'une campagne d'essais exhaustive réalisée sur des pales en aluminium dans des conditions pertinentes pour le givrage des éoliennes.

La deuxième phase de la recherche applique la méthodologie validée à l'évaluation de systèmes passifs de protection contre le givrage. Des essais comparatifs réalisés sur des surfaces en aluminium, en gelcoat et sur un revêtement glaciophobe fournissent des données permettant d'analyser l'influence des propriétés de surface sur l'adhérence de la glace et les mécanismes de détachement. Les résultats de cette recherche mettent en évidence un contrôle stable des paramètres climatiques, des morphologies d'accumulation de glace réalistes ainsi que des comportements de fracture cohérents avec ceux rapportés dans la littérature et observés en conditions réelles. Les valeurs de résistance d'adhérence de la glace présentent un bon accord avec celles obtenues avec des montages expérimentaux d'échelle comparable, tandis que les mesures de résistance cohésive renseignent sur les mécanismes de détachement de la glace qui ne peuvent être capturés seulement par mesures d'adhérence. Une réduction marquée de la résistance d'adhérence est également observée pour les surfaces recouvertes. Cette observation met en évidence une transition d'un mode de rupture principalement adhésif à petite échelle vers des modes de fracture cohésifs ou mixtes dans le cas d'accumulations de glace réalistes à grande échelle. Dans l'ensemble, ce travail établit une approche expérimentale robuste pour l'évaluation de systèmes passifs de protection contre le givre destinés aux applications éoliennes. Les résultats ouvrent la voie au développement de futures stratégies d'atténuation du givrage pour les parcs éoliens en milieux nordiques.

SUMMARY

Atmospheric icing on energy infrastructure has become an important research topic in recent decades. Its impact is particularly significant for wind energy systems operating in cold climates. Under icing conditions, supercooled water droplets can accrete as ice on turbine blades, altering their aerodynamic performance and reducing power production efficiency. These ice accretions may lead to substantial annual energy losses and increased operational challenges for wind farm operators. In response to this issue, considerable research efforts have been directed toward understanding icing mechanisms and developing effective ice protection strategies for wind turbine blades.

This project aims to develop and validate a large-scale experimental methodology for the characterization of atmospheric icing and passive ice protection systems on wind turbine blades for wind farms operating in cold climates. Considering the limited availability of experimental data obtained under realistic and controlled icing conditions at representative scales, this research provides an in-depth experimental framework to bridge the gap between laboratory-scale measurements and field performance.

This study is organized in two main phases. The first phase focuses on the completion and calibration of a large-scale rotating-blade test bench installed in a controlled icing environment. Key governing parameters are measured and characterized to ensure proper repeatability and representative icing conditions. The ice adhesion test procedure developed is based on centrifugal ice shedding and a dedicated ice cohesive strength measurement apparatus which is used jointly with the main rig to further improve the interpretation of the partial ice shedding events observed on the test bench. The reliability and repeatability of the experimental procedure are assessed through a comprehensive test campaign conducted on aluminum blades under conditions relevant to wind turbine icing.

The second phase of the research applies the validated methodology to the evaluation of passive icing protection systems. Comparative tests on aluminum, gelcoat, and an icephobic coating provide data-driven insight into the influence of surface properties on ice adhesion and shedding behavior. The results of this research highlight stable control of the climatic parameters, realistic ice accretion morphologies, and fracture behaviors consistent with those reported in the literature and observed in field conditions. Ice adhesion strengths show good agreement with experimental setups of approximately the same scale, while the cohesive strength measurements provide additional insight into ice detachment mechanisms that cannot be captured by adhesion measurements alone. A marked reduction is also observed in adhesion strength and highlights a shift from predominantly adhesive failure at small scale to cohesive or mixed fracture modes under large-scale, realistic ice accretions. Overall, this work establishes a robust and scalable experimental approach for evaluating passive ice protection systems for wind energy applications. The findings pave the way for future icing mitigation strategies for cold-climate wind farms.

TABLE OF CONTENTS

LIST OF FIGURES

LIST OF TABLES

DÉDICACE

Ce travail est dédié à ma famille, mes amis et toutes les personnes qui, sans relâche, m'ont supporté au travers de ces deux années d'efforts. Le doute qui m'habite constamment est imperceptible grâce à leur présence.

Ce travail est dédié à l'avancement de l'ingénierie et des sciences environnementales qui façonnent l'avenir de notre planète en un horizon plus vert. Dans ce monde où la technologie gruge les ressources existantes, l'innovation équilibrée et responsable est le seul futur viable.

Ce travail est dédié à ceux qui se questionnent, expérimentent et persévèrent, convaincus que le progrès n'a de sens que s'il respecte l'humain et l'environnement.

ACKNOWLEDGEMENTS

I would like to express my deep gratitude to my supervisor, Gelareh Momen, for offering me the opportunity to work on this project and for providing insightful guidance throughout the development of this research. Her expertise, patience, and constant support were essential to the successful completion of this work.

My sincere thanks also go to my co-supervisors, Derek Harvey and Éric Villeneuve, whose thoughtful remarks, technical advice, and availability greatly enriched the quality of this research. Their contribution was essential, and this work could not have been completed without their involvement.

I am grateful to Patrice Rondeau, Luc Chatigny and Carol Mercier for the constant help they provided to materialize this major endeavor. Their input and collaboration were more than valuable; they were an integral part of the countless tests and trials that led to the completion of this project. The technical knowledge and work ethic they taught me constitute key qualities for every step my upcoming professional career.

My appreciation extends to the members of the Anti-Icing Materials International Laboratory (AMIL) and LARGIS, whose collaboration and discussions created an enriching research environment. Special thanks to Ghazal Minoofar and Fateme Eslampanah for their scientific competence and collaboration in our joint project. Their availability and participation during experimental testing and data collection were outstanding.

I gratefully acknowledge the financial support provided by Pattern Energy, PRIMA Québec and ALLIANCE CRSNG, without which this work would not have been possible.

Finally, I wish to extend my heartfelt thanks to my family and friends, whose encouragement, patience, and unwavering support carried me through the challenges of this project. Their presence and trust in my capabilities made this journey both possible and meaningful.

CHAPTER 1

GENERAL INTRODUCTION

1.1 Context of the study

The precarious equilibrium that sustains life on Earth is governed by a continuous and delicate balance of energy. At every scale, energy is exchanged through complex natural processes, transformed between heat, pressure, and movement before ultimately dissipating as heat. This perpetual exchange is mainly driven by solar radiation and gravitational forces, which warm the planet, generate atmospheric circulation, and allow the development of life. Human societies evolved fully within this system and have progressively learned to manipulate energy flows through technology, allowing energy to be harvested, converted, and transported to support daily activities in cities and communities.

However, not all energy sources are renewed at a pace compatible with human consumption. Non-renewable resources, once extracted and transformed, require geological timescales to regenerate, making their depletion inevitable at the scale of human development. In contrast, renewable energy sources are continuously maintained by persistent natural forces, most notably the Sun. Wind energy, for example, arises from large-scale air mass movements caused by atmospheric temperature and humidity gradients induced by the Sun's heat. As a result, renewable energies offer a sustainable alternative, with the added advantage of significantly lower greenhouse gas emissions compared to fossil fuels.

In recent years, renewable energy technologies have progressed rapidly to meet the growing global demand for energy while limiting environmental impacts. This transition has stimulated extensive research efforts and renewed interest in expanding wind energy deployment, particularly in northern and cold-climate regions where wind resources are abundant and high in energy due to increased air density in cold temperatures. Ensuring energy diversity and efficiency in these regions is critical, not only to secure reliable power generation, but also to maximize the performance and longevity of infrastructure operating under harsh environmental conditions.

Among renewable energy sources, wind power has emerged as one of the most proven, scalable, and cost-effective solutions for large-scale electricity production. Modern wind turbines can deliver significant energy output with a comparatively low environmental footprint, making wind energy a pillar of current and future decarbonization strategies. However, the increasing deployment of wind turbines in cold and remote regions introduces new operational challenges that must be addressed to fully use their potential.

Atmospheric icing on wind turbines remains one of the most critical of these challenges. Ice accretion on rotor blades degrades aerodynamic performance, reduces energy output, increases mechanical loads, and may force prolonged shutdowns. Addressing this issue requires a detailed understanding of ice formation, adhesion, and shedding mechanisms under realistic operating conditions. It is within this context that the present work focuses on the development and validation of a large-scale experimental test platform designed to reproduce atmospheric icing on rotating wind turbine blades and to evaluate passive ice protection strategies in a controlled yet representative environment.

1.2 Problem Statement

Wind energy has become a cornerstone of the global transition toward low-carbon and sustainable power generation. Wind turbines offer a renewable and scalable technology with limited greenhouse gas emissions while supporting versatile energy production. Their deployment has expanded rapidly over the past decades, particularly in regions seeking to diversify their energy mix and reduce reliance on fossil fuels and non-renewable energy sources.

Most of the time, cold and northern regions, characterized by vast open spaces and strong, consistent wind resources, are especially well suited for wind energy development. For rural and remote areas with challenging climatic conditions, wind power represents an attractive solution to enhance energy autonomy and resilience. Additionally, wind power performs particularly well in cold temperatures and during winter. Cold air is denser than warm air, which means that, at the same wind speed, it contains more energy and can exert greater force on the turbine blades. Furthermore, winter winds are often stronger and more consistent, increasing the amount of power that can be produced. Together, these factors make cold-climate environments especially favorable for wind energy generation. However, these same environments expose wind turbines to severe atmospheric conditions, including frequent icing events, which pose major operational challenges for wind farms.

Under optimal conditions, wind turbines operate with high aerodynamic efficiency. Their performance is highly dependent on the precise geometry and surface condition of the blades, which are carefully designed to maximize lift and minimize drag. Any modification to the blade aerodynamic profile inevitably leads to power losses and increased mechanical loads, consequently reducing the turbine's functional lifespan. In cold climates, atmospheric icing alters the blade surface through ice accretion, disrupting airflow, degrading aerodynamic performance, and causing significant reductions in energy production. In severe cases, icing can also induce vibrations, imbalance, increased fatigue loads, and safety risks related to ice shedding.

Mitigating these effects is particularly complex due to the large scale, height, and remote location of modern wind turbines. Unlike aircrafts, which can be routinely inspected and de-iced on the ground, wind turbines operate continuously in harsh environments where access is limited, costly, and often impractical. As a result, conventional de-icing approaches used in aviation cannot be directly applied to wind farms, highlighting the need for alternative icing protection strategies.

Consequently, understanding the mechanisms governing ice accretion and adhesion on wind turbine blades is a critical challenge for improving turbine reliability and performance in cold climates. A detailed study of ice adhesion is therefore essential to the development and evaluation of effective icing protection solutions particularly passive approaches aimed at reducing ice adhesion and facilitating ice shedding.

1.3 Literature Review

Atmospheric icing is a phenomenon that affects many aspects of daily life in cold-climate regions, often without being fully noticed by those who experience it. Each winter, specific meteorological conditions lead to the formation and accumulation of ice on exposed surfaces such as roads, buildings, power lines, communication towers, and transportation infrastructure. While sometimes perceived as a temporary inconvenience, atmospheric icing can have significant structural, economic, and safety consequences.

Although icing has always been present in northern climates, its large-scale scientific investigation intensified with the expansion of major energy infrastructures in cold regions. In Quebec, for instance, the rapid development of hydroelectric facilities and extensive high-voltage transmission networks brought increased attention to ice-related structural loading. The 1998 “Ice Storm Crisis” in eastern Canada highlighted the vulnerability of energy systems to freezing rain events and triggered substantial research efforts aimed at better understanding ice accretion mechanisms and their impacts on infrastructure reliability [1].

From a physical perspective, ice is a particularly problematic material. Under appropriate atmospheric conditions, supercooled water droplets can freeze upon impact with exposed surfaces, forming strongly adherent ice layers. Ice not only bonds effectively to a wide variety of materials, but it also has significant mass, which can generate considerable mechanical loads on structures. In systems that rely on aerodynamic performance, such as aircraft or wind turbines, ice accretion is especially detrimental because it modifies surface geometry and roughness. Even relatively small changes in shape can significantly alter aerodynamic forces, therefore degrading performance and efficiency.

Icing events occur under specific combinations of air temperature, humidity, liquid water content, wind speed, droplet size, and precipitation type. These meteorological parameters govern both the rate of ice accumulation and the physical characteristics of the accreted ice. Such conditions are common during winter in many cold and coastal regions, making atmospheric icing a recurring and predictable operational challenge for exposed infrastructure.

Within this broader context, wind turbines are particularly vulnerable due to their large rotating blades and continuous exposure to the atmosphere. The development of this test method is therefore oriented towards icing caused by freezing rain, which is one of the most detrimental meteorological events for wind turbine icing [2].

Some of the key parameters that allow to describe icing events are liquid water content (LWC) in the air, wind speed, relative humidity, precipitation intensity, water droplet size, air temperature and of course the duration of the event. The problem of wind turbine icing resides in the fact that while rotating in icing conditions, the blades accumulated ice on their leading edges due to supercooled droplets colliding with them. This causes a gradual modification of the aerodynamic profile and surface finish of the blades, which results in increased drag, decreased lift and overall loss of efficiency and energy production. In some cases, icing can completely halt wind farm output power during severe events, with an average production loss of 16% during winter in certain regions [3]. A geographical survey found that coastal areas of Newfoundland, southeastern Quebec, and the Maritimes are among the most promising regions for wind energy because of their constant winds and colder, denser air. However, they present high prevalence of icing, hence the importance of icing mitigation systems [4]. In these regions, it can take several days, even weeks, before a turbine can restart again. In fact, the most common way of dealing with the effects of severe icing storms is to wait for the blades to shed their ice naturally by the effects of solar radiation, ice erosion and aging, which is particularly costly due to lack of production. Return to a normal production state can be accelerated using ice removal, active deicing systems or passive ice protection systems, but the efficient solutions represent a considerable investment and are not always reliable [5]. This justifies the present study which aims at accelerating the development and improvement of these protection systems, which could lead to more affordable, reliable and widespread solutions for this problematic. In addition to energy loss, icing causes vibrations and accelerated wear on turbine blades, leading to increased maintenance costs. It also poses safety hazards due to ice shedding [1]. To mitigate these impacts, industry seeks to minimize these effects through efficient de-icing strategies, particularly given that wind turbine efficiency at converting mechanical energy to electricity is already limited in optimal conditions [6].

Atmospheric icing of wind turbines, particularly in northern regions, presents a substantial challenge to the wind energy industry. Ice accumulation on turbine blades significantly impacts energy production, turbine efficiency, and overall structural integrity [1]. Research on wind turbine ice protection systems has increased significantly in the recent years as the demand for wind farms in cold regions increased as well and icing problematics become more frequent and unpredictable due to the effects of climate change. Hence, the development of these systems require innovative technologies and testing environments to adequately replicate these dynamic events. Icing events in nature are sporadic conditions which makes field tests difficult to organize. To help and accelerate the development of ice protection systems for wind energy and aeronautical purposes large scale laboratory test setups and environment are necessary.

For atmospheric icing, air relative humidity, the amount of liquid water suspended in the air, air and surface temperature, wind speed, droplet size, and even solar radiation are all key parameters governing its formation and determining the resulting ice types. The two main type of ice that may accumulate on structures are glaze ice and rime ice [2]. Glaze ice is usually obtained for droplets of large diameter, temperatures above –5 °C, relative humidity above 90%, and supercooled droplets that do not freeze immediately upon impact. The resulting ice is dense, translucent, and adheres strongly to the surface. It is generally considered as more problematic since its occurrence frequency is high thanks to the more probable mix of meteorological conditions than can lead to its formation. It also generally exhibits higher adhesion strength and has a more significant impact on the aerodynamic profile of the surface on which it accretes compared to rime ice. In contrast, rime ice forms under low relative humidity and cold temperatures, below –10 °C, and the typically small, supercooled droplets freeze instantly upon impact. Although often less dense and more brittle, this type of ice produces very thick and irregular accretions. In both cases, ice accumulation significantly affects the aerodynamic profile of the rotor and the surface roughness, resulting in increased drag and lower lift forces which drastically reduce the power production of a wind turbine.

Furthermore, ice predominantly accumulates on the leading edge of a rotor when an icing event occurs while the wind turbine is in operation [3]. Rime ice tends to spread further along the blade chord and sometimes even toward the trailing edge. Meteorological conditions also influence the persistence of an iced surface after an icing event. Ice may remain for several weeks in certain scenarios [4], leading to substantial production losses. It is important to keep in mind that the two ice types discussed above represent the extremes of a complex spectrum of icing conditions, which may also include wet-snow accretion; therefore, ice properties vary considerably as meteorological conditions change [5]. Furthermore, the complexity of wind turbine icing is amplified by the range of operational states in which turbines may be found at the time of an icing event. Turbines may be operating at rated rotational speed or remain idle due to maintenance or system malfunctions. Such differences in blade motion alter local flow conditions and droplet impingement characteristics, leading to distinct ice accretion patterns and shapes. This makes close meteorological monitoring and precisely tailored icing protection systems mandatory for effective prevention of wind farm down times. For these reasons, wind-energy production sites must be equipped with accurate icing-detection methods.

Various tools are used to obtain data that allow estimation of on-site meteorological conditions. More specifically, to detect conditions conducive to atmospheric icing, the use of dual anemometry combined with relative humidity measurements is recommended [6] to identify the presence of an icing event on a wind-farm site. The intensity of the icing event can be assessed using the turbine power curve, video monitoring, ice sensors, or ice-density sensors. It is recommended that all meteorological measurement instruments be installed on a tower at an elevation corresponding to the center-height of the rotor, on the nacelle of the turbine. Dual anemometry is an icing-detection technique that relies on a threshold applied to the difference in wind speed measured between a standard anemometer and a heated anemometer placed close to one another, in order to determine whether icing is occurring.

Unlike the standard device, the heated anemometer does not retain ice and can therefore make an ice-free wind speed measurement. Dual anemometry is a measurement method that leaves some discretion to the user regarding the choice of threshold for the wind-speed difference; however, in general, Ilinca and Parent report [6] that a value of 5% provides reliable results and prevents exclusion of weaker icing events.

Relative humidity measured below 0°C is also crucial for detecting icing episodes and is more commonly used than dew-point measurement [7]. However, relative humidity below 0°C does not correlate reliably with ice accumulation; relative humidity above 95% has been observed below 0 °C without any ice forming on structures at heights exceeding 80 m. Overall, it is recommended to detect icing events by relying on multiple indicators, such as those discussed above, to minimize erroneous detections.

To this end, additional icing-measurement techniques may be considered. Among others, visibility measurement, reflecting cloud density, can be useful, and the use of meteorological predictive models as well as precipitation sensors for detecting freezing rain are also recommended [6].

1.4 Current Icing Protection Systems

Current icing protection technologies are generally classified as active or passive. Active methods, which require energy input, are currently the most effective in the industry. These methods involve heating elements or hot air circulation inside the blades to melt the ice [8], this principle is called de-icing, as it operates reactively by removing ice that already accumulated on the blade, most often on its leading edge. On the contrary, active solution can also be used as anti-icing methods which are used proactively and aim to prevent the accumulation of ice on the blade. However, the energy consumed by active de-icing systems detracts from the energy generated by the turbine itself, with de-icing the blade tips requiring up to four times more energy than the base of the blade [9]. Studies have demonstrated that selective heating of the most critical sections of the blade can reduce energy use by targeting the most aerodynamically significant areas [10]. On the other hand, passive methods, such as hydrophobic or ice-phobic coatings, aim to lower ice adhesion without consuming energy [6]. While promising, these coatings have limitations, including a lack of durability and decreased effectiveness against all forms of icing. Regular reapplication of coatings is required, increasing maintenance costs [12]. Furthermore, coatings may increase the risk of ice shedding, posing hazards to nearby structures and personnel.

Several innovative de-icing approaches are under investigation. Flexible blades, designed to mechanically break ice under wind force, and the use of microwave technology to heat the blade surface are among the emerging methods [6]. One particularly promising approach is the use of hybrid de-icing systems, which combine passive coatings with active heating elements. These systems leverage the strengths of both icing protection technologies: active heating is used to de-ice the blade by melting ice accreted on the leading edge, while the passive coating helps prevent the melted water from refreezing as it flows along the blade's profile. Hybrid technology development strongly relies in the development of tests that allow for accurate optimization of the heated zones and coherent use of the ice-phobic and hydro-phobic coatings. One study by Villeneuve et al. [13] showed that coating a turbine rotor with an ice-phobic material, while heating the leading edge, reduced de-icing energy consumption for complete de-icing of the blade by 44%, which is highly promising for the continuation of research in this field.

As much as test platforms have the added benefit of real-world representativity and accurate representation of the complex atmospheric icing adherence mechanisms, numerical simulations also play a critical role in optimizing de-icing strategies. Such tools allow research teams to obtain clear results and statistically representative sample sizes shorter time spans. However, the complexity of computational codes associated with fluid–structure or fluid–solid–structure interaction simulations represents a significant numerical challenge. This continuously advancing technology is particularly well suited for simulating ice accretion, as the process inherently involves multiphase interactions between air of varying thermodynamic properties, liquid or solid precipitation, and solid structures such as wind turbine blades. By employing an approximate ice geometry representative of rime ice conditions in combination with a thermal simulation, it is possible to estimate key parameters, including the energy required for blade de-icing. A study reported that such an approach predicts de-icing energy demand with an error of less than 10% compared to experimental measurements [11].

Using an approach based on the energy balance governing the freezing of water droplets, Fortin demonstrates the ability to simulate ice accretion on a two-dimensional object for both dry and wet regimes, achieving an accuracy of 80% in reproducing aerodynamic and gravitational effects, as well as generating ice shapes sufficiently close to those obtained experimentally [2]. Numerical simulations therefore constitute a growing field of interest in icing research and may eventually allow for full three-dimensional reproduction of icing phenomena.

1.5 Challenges in Testing and Ice Adhesion Theory

Understanding the mechanisms of ice adhesion is crucial for developing effective de-icing technologies. Ice adhesion strength depends on factors such as temperature, surface properties, and the type of ice. A study by Andrews and Lockington [12] showed that ice fractures differently depending on the temperature, with cohesive fractures occurring at lower temperatures (-20ºC) and adhesive fractures near the melting point. This information is key for designing coatings that minimize ice adhesion and maximize ice shedding.

Indeed, it was shown that, in general, the fracture energy of ice at low temperatures and high density, closer to the density of liquid water, is higher and is also characterized by a cohesive fracture mode, classically leaving a clean break on the surface of the substrate. As temperatures approach the melting point of ice, the fracture energy decreases significantly, and the observed fracture becomes predominantly adhesive, meaning that the ice detaches from the substrate wall in intact blocks. This phenomenon is associated with the formation of a liquid-like layer between the substrate and the ice and can be accelerated by the addition of solutes within the ice. Ice may also detach in a fracture mode dominated by adhesion but without the presence of this liquid-like layer, especially over small surface areas. In such cases, it has been shown that detachment may be governed either by stress or by toughness.

Contrary to some assumptions, detachment does not occur when the average shear stress exceeds a critical value, but rather when the critical stress is exceeded over threshold area at the interface between the ice and the substrate [13]. Experiments must be carried out with caution, as the timescales associated with detachment are extremely short.

In the case of freezing rain, which leads to a large number of severe icing events documented in wind farms, the study of surface wetting is relevant, particularly for the development of hydrophobic coatings. Whether a surface becomes wetted or not, which directly influences whether freezing rain accumulates or is shed at impact, depends on a delicate balance between the internal forces of water droplets and the ability of the coated surface to limit their effect on surface tension. This is generally achieved by reducing the size of droplet contact points on the substrate [14].

One thing is certain: although many studies have explored the topic of ice adhesion in depth, measured stress values still vary considerably depending on testing parameters and environments. For adhesion on metals, the maximum stresses reported span from 0.07 MPa to 9.3×10^{-4} MPa for the same type of test [15].

1.6 Current Experimental Testing Methods

Testing de-icing methods at different scales also presents challenges. Small-scale tests, such as push-off and centrifugal adhesion tests, provide valuable insights into ice adhesion properties [16], but large-scale tests, such as those conducted in wind tunnels, are necessary to replicate real-world conditions. The reliability of accumulated data will always be limited by the degree of replicability and the ability of experimental setups to adequately represent natural phenomena. Typically, the wind energy industry relies on field tests conducted on actual infrastructures to validate the real performance of de-icing systems. However, such field testing is often very costly and complex to implement, especially when it requires modifications to existing structures [17]. Field tests are also entirely dependent on meteorological conditions, which prevents guaranteeing the occurrence of specific icing events and can significantly extend the duration of a study.

This is why intermediate-scale testing becomes relevant, as it can reproduce the real behavior of rotors as closely as possible within a controlled environment. This level of testing enables reliable characterization of de-icing methods at lower cost while remaining representative of field conditions. The AERTS (Adverse Environment Rotor Test Stand) rig at Pennsylvania State University represents such an installation. It includes a horizontal rotor of approximately 3 m in diameter placed inside a controlled and instrumented icing chamber, thereby replicating the behavior of a wind turbine operating in icing cloud conditions [18].

This setup, equipped with a slip ring for supplying electrical power to the rotor, has notably been used to determine the minimum ice thickness required to trigger natural shedding as a function of blade section and applied de-icing power [19]. It has also enabled the development of a heating control sequence adapted to temporally varying icing conditions [20].

A comparable facility, the DLR Whirl Tower, is dedicated to full-scale icing experiments on medium-sized helicopters. This vertical-axis setup enables the evaluation of electrothermal de-icing systems under dynamic loading conditions and accommodates testing in freezing rain and mixed-phase precipitation. However, the vertical configuration employed in both of these test benches may yield ice accretion patterns that are less representative of those encountered by wind turbines, given the influence of precipitation direction. Advancing ice adhesion characterization through large-scale centrifugal testing on a horizontal axis could therefore provide more realistic insights for optimizing wind turbine anti-icing technologies, underscoring the rationale for developing the test bench presented in this study. In this type of test infrastructure, controlling the icing parameters is extremely important.

At smaller, yet still intermediate, scales, two complementary experimental approaches have been developed to investigate ice adhesion and de-icing performance under dynamic conditions. The centrifugal adhesion test (CAT) is based on measuring the centrifugal force required to detach ice from a coated substrate. The setup typically consists of a small rotor equipped with two blades to ensure dynamic balance. Ice test specimens are mounted at a known radial distance, and the rotational speed at the moment of ice detachment is recorded [21]. From this speed, the applied centrifugal force and then the apparent ice adhesion strength can be calculated. While this method provides a relatively simple and repeatable means of quantifying adhesion, it is generally conducted at small scale and outside of realistic icing cloud conditions, limiting its representativeness with respect to full rotor aerodynamics.

A more advanced configuration inspired by this principle is the Spinning Rotor Blade (SRB) test bench developed at LIMA to address icing issues in the aeronautical sector [22]. Unlike conventional static wind tunnel experiments, which are typically limited to two-dimensional ice accretion studies [23], the SRB setup operates within a wind tunnel and simulates the motion of a rotating blade through an icing cloud. This configuration enables more realistic reproduction of the aerodynamic and thermodynamic conditions experienced by rotating lifting surfaces. The SRB facility has also been equipped with integrated heating elements, enabling the evaluation of hybrid de-icing strategies combining icephobic coatings with active electrothermal heating [24]. Furthermore, the installation includes high-speed cameras, allowing detailed observation of ice fracture and shedding mechanisms under realistic loading scenarios.

Although the CAT and SRB configurations represent significant advancements over purely static adhesion tests, they remain limited in rotor diameter and in the range of controllable icing parameters. Consequently, a gap persists between small-scale adhesion characterization and large, fully representative wind turbine testing. Bridging this gap through the development of a horizontally oriented, larger-scale centrifugal test bench operating under controlled icing conditions would enable more comprehensive investigation of ice accretion, adhesion, and hybrid protection strategies. This need directly motivates the development of the experimental infrastructure presented in this study.

In conclusion, the development of more energy-efficient de-icing systems is essential to reduce the operational costs of wind farms in cold climates. While active de-icing methods are currently the most reliable, their energy demands highlight the need for more sustainable solutions. Even if some hybrid icing protection systems are promising, testing methods for these protection systems are still lacking the scale factor that can help highlight key elements of their functioning. Advancing ice adhesion characterization through centrifugal testing and large-scale test benches could significantly help researchers optimize anti-icing systems for wind turbines. By providing a better understanding of the complex interactions affecting ice adhesion during atmospheric icing events, this body of research also contributes invaluable insights into enhancing the efficiency and reliability of wind energy systems.

1.7 Research Objectives

This research project consists of two main phases. In the first phase, the study focuses on developing and validating a robust, repeatable, and high-precision test rig and methodology for the quantitative characterization of ice accretion and shedding mechanism on representative rotating blades. The test rig and methodology developed will also allow to assess the anti-icing and de-icing performance of passive icing protection strategies. This phase establishes reliable experimental protocols, measurement techniques, and performance metrics that ensure consistent and meaningful assessment under controlled and representative icing conditions. To achieve this, the targeted objectives are:

- To complete the development of a large-scale test bench and perform a comprehensive calibration of the test conditions by evaluating key governing parameters including temperature, LWC, median volume diameter (MVD), and precipitation intensity;

- To create an efficient test procedure for centrifugal ice adhesion testing in the ranges of the established key parameters;

- To incorporate an ice cohesive strength measurement apparatus into the test procedure to increase the accuracy of the measurements;

- To assess the reliability and repeatability of the results yielded by the test rig and procedure developed with a comprehensive test campaign on rotating aluminum blades in conditions relevant to wind turbine icing.

Building upon the developed and validated test methodology, the second phase of the project aims to further advance the study of the large-scale experimental test bench and ensure its relevance and applicability to the wind turbine industry. In this phase, the performance of a selected passive icing protection system will be evaluated using the developed test method, enabling comparative analysis and providing insights into their effectiveness, limitations, and potential for real-world implementation. This second part of the project aims to:

- To generate data-driven insights into the performance of various substrates under controlled conditions.

- To validate the reliability and robustness of the test method for future icing protection systems testing.

Ultimately, this research aims to establish a robust, standardized and scalable approach for evaluating wind turbine icing, shedding mechanism and passive icing protection systems under conditions representative of wind energy applications. The findings will contribute to the development of more effective anti-icing and de-icing strategies, enhancing wind turbine performance and reliability in cold climate region.

1.8 Methodology

To attain the objectives defined in the previous section, a rigorous and structured methodology needs to be developed and followed throughout the completion of this research project. Given the experimental nature of the work and the evolving state of the experimental infrastructure, the adopted methodology reflects both a systematic scientific approach and the practical realities associated with large-scale atmospheric icing experiments. The sequence of steps described below is established by the research team as an optimal framework to guide the investigation toward conclusive and reliable outcomes within the scope of this master's project.

The first step of the methodology consists of conducting an extensive literature review on atmospheric icing, wind energy in cold climates, and the operational challenges associated with ice accretion on wind turbine blades. Existing ice adhesion measurement techniques and test benches are evaluated in detail, as is scaling effects between laboratory and field conditions, and the limitations of small-scale experimental approaches. This review, presented in section 1.6 of this thesis, serves as the foundation for identifying knowledge gaps and defining the scope of the investigation.

Based on this analysis, the scope of work is refined to focus on the development and validation of a large-scale experimental methodology capable of producing representative ice accretion and adhesion measurements on rotating blades under controlled atmospheric icing conditions. The work is structured in two main phases: first, the development and characterization of the experimental platform and test procedure using aluminum reference blades, and second, the application of the validated methodology to the evaluation of passive icing protection solutions.

Following the definition of the scope, the governing physical parameters influencing ice accretion and adhesion are identified. Among the numerous variables reported in the literature, four parameters are retained as critical and are controlled and characterized in this work: air temperature, liquid water content (LWC), median volume diameter (MVD), and precipitation intensity. Test conditions are defined to target atmospheric icing events relevant to wind turbine operation in cold climates, with particular emphasis on conditions leading to strong ice adhesion and mechanically significant ice accretions.

An initial phase of experimental work is dedicated to assessing the baseline performance of the facility, identifying limitations in parameter control, and evaluating measurement uncertainties. This characterization phase highlights the need for additional sensors and improved control of key environmental parameters. As a result, significant effort is devoted to the integration and calibration of instrumentation dedicated to temperature regulation, liquid water content (LWC), median volume diameter (MVD), and precipitation monitoring.

In parallel with the test chamber characterization, dedicated techniques are implemented to quantify the ice properties required for adhesion analysis. High-speed imaging is used to observe ice accretion and shedding events in real time, providing insight into detachment mechanisms and fracture initiation. Three-dimensional scanning is introduced as a critical measurement tool to accurately determine ice accretion geometry and post-shedding ice distribution on the blades. This information is used to identify the effective shedding areas required for the calculation of adhesion stress. While the detailed implementation of these methods is presented in the associated papers, their integration into the experimental workflow represents a key element of the present methodology. In addition, an auxiliary setup is incorporated to characterize the cohesive strength of the accreted ice, allowing differentiation between adhesive, cohesive, and mixed failure modes during shedding events. The iterative development process that led to these upgrades, which included multiple calibration and verification campaigns, was necessary to transform the test bench into a quantitative experimental platform suitable for repeatable ice adhesion measurements.

Once the test bench and measurement systems are fully characterized, a standardized experimental procedure is established. This procedure defines the sequence of operations for ice accretion, stabilization, centrifugal loading, ice shedding observation, and post-test measurements. Special care must be taken to ensure consistency in blade preparation, environmental conditioning, and data acquisition.

Aluminum blades are used as a reference substrate to validate both the test bench and the experimental procedure. With these blades, a benchmarking campaign is conducted under controlled and repeatable icing conditions to assess the reliability and repeatability of the measured adhesion values. The results are compared with values reported in the literature and analyzed in terms of fracture modes and scaling behavior as presented in the first paper of this thesis. This validation phase will confirm the robustness of the methodology and establish aluminum as a reliable baseline for eventual comparative studies.

Once validated, the methodology developed is applied to the evaluation of selected substrates representative of passive icing protection strategies. Tests must be conducted under identical conditions to ensure direct comparability with the reference case. The collected data should then enabled assessment of the influence of surface properties on ice adhesion and shedding behavior and support extrapolation toward large-scale and field-relevant conditions, as presented in the second paper shown in this work.

As this work proves, the experimental process is marked by several challenges inherent to the study of atmospheric icing. Ice accretion and adhesion are found to be highly sensitive to small variations in environmental conditions, requiring extensive trial-and-error during parameter tuning and procedure building. Depending on the target conditions, individual tests could range from one day to more than a week in duration. To address these challenges, a systematic and iterative approach is adopted, emphasizing careful calibration, progressive adjustments, and thorough documentation of test conditions. These efforts are essential to improve the overall robustness of the methodology and deepening the understanding of ice adhesion behavior at large scale.

1.9 Thesis outline

This thesis is divided into seven main parts. The general introduction starts by presenting the scientific and industrial context of the study and introducing the research problem related to atmospheric icing on wind turbines in cold climates. Then, the literature review summarizes the current state of knowledge on atmospheric icing, ice accretion and adhesion mechanisms, and existing ice mitigation strategies for wind energy applications, while identifying the main gaps that need to be addressed in this work. The research objectives section defines the goals of the study and explains how they respond to the identified challenges. The methodology describes the experimental approach developed throughout the project, including the characterization and instrumentation of the icing test bench, the definition and control of key physical parameters, and the establishment and validation of the ice adhesion test procedure. The work follows through with the first article which focuses on the development, calibration, and validation of the large-scale rotating test bench and the centrifugal ice adhesion test under controlled icing conditions. Then, the second article applies the validated methodology to the evaluation of passive icing protection systems and compares the ice adhesion and shedding behavior of different substrates relevant to the industrial partners of the project. Finally, the general conclusion summarizes the main results of the thesis, discusses the limitations of the work, and proposes perspectives for future research.

CHAPTER 2

A Large-Scale Rotor Test Platform for Atmospheric Icing Simulation and Passive Ice Protection Evaluation

2.1 Paper Presentation

The article entitled “A large-scale rotor test platform for atmospheric icing simulation and passive ice protection evaluation” presents the design, calibration, and validation process of a novel large-scale experimental test bench dedicated to the study of atmospheric icing on wind turbine blades. The platform consists of a horizontal-axis rotor installed in a refrigerated chamber, allowing controlled reproduction of representative icing conditions encountered by wind turbines operating in cold regions. The study introduces a centrifugal ice adhesion testing methodology combined with detailed characterization of icing parameters, including temperature, liquid water content (LWC), median volume diameter (MVD), and precipitation intensity.

The primary scientific contribution of this work lies in bridging the gap between small-scale laboratory ice adhesion tests and full-scale field observations. Unlike conventional vertical-axis or small-rotor setups, the proposed test bench enables the investigation of ice accretion and shedding mechanisms on rotating blades at a scale that captures both adhesive and cohesive fracture phenomena. The integration of a dedicated ice cohesive strength measurement apparatus deepens the test methodology by allowing partial detachment events to be properly analyzed, improving the accuracy of ice adhesion strength evaluation.

The results obtained using aluminum blades demonstrate good repeatability and consistency with values reported in the literature and on other reference test benches. This validation establishes the platform as a robust tool for studying ice adhesion under realistic and reproducible conditions at a larger, more representative scale. This article directly addresses some of the core objectives of the master's research project. It corresponds to the first phase of the work, which focuses on completing the development of the experimental test bench and establishing a reliable and precise centrifugal ice adhesion test methodology. Specifically, the article contributes to:

1. The calibration and characterization of key icing parameters such as temperature, LWC, MVD, and precipitation intensity;
2. The development and validation of an efficient test procedure for centrifugal ice adhesion measurements;
3. The integration of ice cohesive strength measurements into the adhesion evaluation;
4. The assessment of test repeatability and reliability through systematic testing on aluminum blades under conditions representative of wind turbine icing.
5. A deeper understanding of ice accumulation, ice properties and ice shedding mechanism on aluminum rotating blades.

Additionally, the article prepares the second phase of the thesis by demonstrating that the test bench is suitable for evaluating passive icing protection systems. The article has been published in the journal *Results in Engineering* (Elsevier) and is currently available online on ScienceDirect. It was published in November 2025 and has successfully completed the peer-review process, confirming its scientific validity and relevance to the field of wind energy and atmospheric icing research.

2.2 Paper Manuscript

A Large-Scale Rotor Test Platform for Atmospheric Icing Simulation and Passive Ice Protection Evaluation

Authors: Thomas Allard[1], Derek Harvey[1], Éric Villeneuve[2], Adrian Ilinca[3] and Gelareh Momen[3,T].

Affiliations: [1]Department of Applied Sciences, University of Québec in Chicoutimi, [2]Département de mathématiques, informatique et génie de l'Université du Québec à Rimouski, [3]École de technologies supérieures.

Corresponding author: Gelareh Momen.

2.3 Abstract

Ice accumulation on the leading edges of wind turbines significantly reduces energy output, aerodynamic efficiency, and structural integrity. In recent years, research into ice protection systems has intensified, driven by the growing deployment of turbines and rotorcraft in cold climates. However, the development and validation of these systems are hindered by the rarity and unpredictability of natural icing events, making field-testing impractical. To address this, there is a pressing need for large-scale laboratory platforms that can reliably replicate atmospheric icing conditions. This study presents the design and implementation of a horizontal axis rotating-blade test stand installed within a cold room, enabling controlled simulation of representative icing scenarios. Unlike most existing setups, the platform reproduces realistic icing through a complete accumulation-pause-shedding sequence, allowing precise characterization of ice morphology prior to detachment. The procedure leverages centrifugal ice adhesion measurements and is validated using a metallic substrate to ensure repeatability and comparability with prior studies and small-scale tests for two specific ice types problematic for wind turbines. The configuration captures both adhesive and cohesive failure mechanisms at a meaningful scale, reflecting fracture behaviors typically observed on full-sized turbine blades. The validation tests show results in accordance with other similar test benches with ice adhesion strength measured at 0,25MPa at -12ºC and 0,15MPa at -5ºC. The cohesive strength of the ice, required for the evaluation of ice adhesion strength in partial detachment cases, is measured specifically for this test bench as well using a dedicated apparatus. The setup is particularly suited for evaluating passive ice protection strategies, such as icephobic surface coatings, under realistic and reproducible conditions. Consequently, it provides a robust foundation for future studies by bridging the gap between small-scale laboratory methods and full-scale field behavior.

2.4 Introduction

The growing demand for wind energy systems in cold climates has renewed interest in the study of atmospheric icing on wind turbine blades. Wind energy has the potential to be highly productive in cold regions due to more intense and constant winds, and denser air [1]. However, ice accumulation alters the effective blade profile, degrading aerodynamic properties, increasing mechanical loads, which translates to substantial power losses, increased maintenance costs and safety concerns. These impacts are particularly severe in northern regions, where prolonged icing events can result in production losses exceeding 20% during the winter months [2]. Even following an icing event, residual ice may remain adhered to the turbine blades for extended periods, up to three weeks in extreme cases, further amplifying production losses.

Ice can accumulate on a surface when supercooled water droplets impact and freeze upon contact. These droplets remain in a liquid state below 0 °C until impact and originate from various sources, including clouds or fog (in the case of small droplets) and freezing drizzle or rain (for larger droplets). Ice typically forms on turbines in two main types: glaze ice and rime ice. Glaze ice, formed near the freezing point of water under high humidity, results in dense, transparent ice that strongly adheres to turbine blades. Rime ice, occurring in colder temperatures, forms a more fragile, opaque layer [3]. Both types affect the aerodynamics of the blades, even though glaze ice is more frequently associated with heavier output losses [4]. In between these two types of ice, mixed ice can be formed, combining characteristics of both types. Studies have shown that certain atmospheric conditions can prolong the presence of ice on turbines, leading to weeks of reduced energy production in extreme cases [5]. Although effective detection methods are crucial for identifying icing events in advance and minimizing power losses [6], prevention alone is insufficient to mitigate the effects of icing on wind turbines, which emphasizes the necessity for specifically designed icing protection systems.

Icing protection methods are generally classified as active or passive. Active methods, which require energy input, are currently the most effective in the industry. These methods involve heating elements or hot air circulation inside the blades to avoid ice formation or melt accumulated ice. Such methods require a high energy demand, especially for de-icing the blade tips that require up to four times more energy than the base of the blade [7]. Studies have demonstrated that selective heating of the most critical sections of the blade can reduce energy use by targeting the most aerodynamically significant areas [8]. Moreover, these methods rely on accurate predictions of icing events to heat up the blades before freezing precipitation appears since their reaction time is generally severely limited. Added to the issue of runback water refreeze, it makes active methods more targeted towards anti-icing than de-icing.

Passive methods, such as hydrophobic or ice-phobic coatings, aim to prevent ice adhesion without consuming energy [6]. Upon impact of the water droplets, these coatings can help delay the liquid to solid transition of the droplets from supercooled state, meaning that water could roll off without freezing if the liquid state can be preserved. This behavior depends on dynamic factors such as impact velocity, droplet size and heat exchange. Nonetheless, if ice still accumulates on the surface, passive coatings can help reduce the adhesion strength of the ice [9]. In the case of wind turbines, this translates to easier and earlier ice shedding after an icing event, resulting in less down time and production losses. While promising, these coatings have limitations, including a lack of durability, decreased effectiveness against all forms of icing, and significant maintenance costs [10], adding to the importance of improved testing capabilities in the development of these technologies.

One particularly promising line of research is hybrid de-icing systems, which combine passive coatings with active heating elements. A study by Villeneuve et al. [11] showed that coating a turbine rotor with an ice-phobic material, while heating the leading edge, reduced de-icing energy consumption by 44%. This study was conducted using the Spinning Rotor Blade (SRB) test bench at the Anti-Icing Materials International Laboratory (AMIL). The SRB is a small-scale rotor system exposed to high wind speed icing conditions within a refrigerated wind tunnel. It provided valuable data on ice adhesion for hybrid protection systems by enabling centrifugal shedding analysis at a constant rotational speed in a controlled icing cloud. Additionally, simulation tools are now more useful in optimizing de-icing systems, with thermal and fluid-structure interaction models achieving unprecedented accuracy [12]. Despite these advances, challenges remain in balancing energy efficiency, durability, and safety across varying climatic and operational conditions—highlighting the need for scalable and reproducible laboratory testing platforms to accelerate development.

Ice adhesion strength depends on factors such as temperature, surface properties, and the type of ice and consequently it is important to experiment under representative conditions of the targeted application. However, testing icing protection systems at different scales presents challenges. Small-scale tests, such as horizontal push-off and centrifugal adhesion tests, provide valuable insights into ice adhesion properties [13]. However, large-scale tests are necessary to replicate real-world conditions where ice failure is typically mixed (involve cohesive and adhesive failure) and observe scale-specific ice fracture mechanics, an inherently complex phenomenon [14]. Such test platforms, like the Adverse Environment Rotor Test Stand (AERTS) at Pennsylvania State University, allow for controlled cloud icing simulations and validation of de-icing techniques [15]. This vertical axis rotor test stand performs well in recreating realistic atmospheric icing scenarios for wind turbines and allows testing for multiple active de-icing technologies. It can be equipped with different blade systems, including a scaled-down section of a wind turbine profile equipped with electrothermal heating. Another comparable test infrastructure, the DLR Whirl Tower Facility, is consecrated to full-scale icing tests of medium size helicopters. This vertical axis test bench supports testing of de-icing systems under dynamic loads and can be used in freezing rain and mixed precipitation scenarios [16]. On the other hand, the vertical axis used in both these test benches can result in less representative ice accumulation for wind turbines in consideration of the direction of precipitation, larger water droplet supercooling and lower rotation speeds. Advancing ice-adhesion characterization through large-scale centrifugal testing on a horizontal-axis platform with long droplet fall distances, as implemented in the present study, enables the formation of supercooled droplets and more realistic wind-turbine icing scenarios. Such an approach can significantly support the optimization of anti-icing and de-icing systems for wind turbine applications, thereby motivating the development of the test bench described here.

Furthermore, ice shedding from wind turbine blades is a complex process influenced by both environmental conditions and variable operational dynamics. Unlike helicopter rotors, wind turbines operate under highly variable conditions: their rotational speed is non-constant, they can be idle during icing events, and they experience precipitation approaching from a broad range of angles. Icing conditions for wind turbines are also highly variable, spanning the full spectrum of atmospheric phenomena including supercooled clouds, freezing fog, freezing drizzle, and freezing rain. As a result, both ice accretion and shedding conditions are more complex and less predictable, making it significantly more challenging to establish reliable icing and ice shedding testing protocols. During low-speed operation, greater ice mass may be required to trigger a detachment. In the absence of intervention, natural de-icing processes such as solar radiation, sublimation, and wind erosion can lead to unpredictably delayed shedding over several days [17]. These factors highlight the need for a controlled test bench that replicates realistic rotational conditions and icing regimes, enabling accurate evaluation of shedding behavior and ice protection strategies.

This paper presents the development of a large-scale horizontal-axis rotor test stand for characterizing atmospheric icing and evaluating passive ice protection systems for wind turbines. The setup enables ice adhesion benchmarking under carefully controlled parameters, including temperature, liquid water content (LWC), median volume diameter (MVD), and precipitation intensity. These parameters are controlled inside a tall, refrigerated chamber in which the test stand is installed. The test stand itself consists of a 2,6m diameter rotor exposed to freezing rain from a water spraying array at the top of the chamber. The experimental protocol focuses on a realistic sequence of ice accumulation on the rotor's leading edges, pause, and forced centrifugal shedding of the ice, allowing precise measurements of ice morphology and adhesion behavior. To complement the adhesion strength evaluation, a cohesive stress test apparatus was implemented to directly measure this condition-dependent parameter, enabling more precise data acquisition. The device consists of small rotating cylinders positioned in the precipitation zone ahead of the rotor, where they accumulate ice under the same conditions. The ice is then subjected to a tensile (traction) test to determine its cohesive strength. Such a combination of testing apparatuses is missing from the literature and could greatly improve global comprehension of the interactions of the cohesive and adhesive properties in regard to the shedding mechanisms of the ice. With its wide range of collected data, this work represents an innovation in the field of icing research as it will allow for rapid, repeatable and realistic characterization of icing protection technologies for wind turbines. It is a step forward in bridging the gap between small-scale laboratory tests and field-scale icing phenomena, advancing the understanding of ice shedding mechanics and how they are influenced by low-adhesion surface technologies. This paper highlights the design of this novel test bench, and the data acquired to validate its performance for evaluating ice adhesion on surface coatings. This paper first describes the control of icing conditions, followed by the test methodology, testing principles, and key results.

2.5 Materials and Methods: Icing Precipitation

2.5.1 Cold Chamber Characteristics

The large-scale test bench is installed in the *Centre international d'ingénierie nordique* (CIIN) largest cold room which stands at 12 meters tall as shown in Figure 2.1. The high ceiling height allows the generation of representative freezing rain droplets, as it provides sufficient time for the droplets to reach a supercooled state and attain terminal velocity before impacting the rotor. The chamber is cooled by a high-capacity ammonia-based system that maintains the test temperature within ±1 °C of the target, from the rotor level to the top of the chamber. The system is capable of reaching temperatures as low as –40 °C and the temperature is closely monitored around the rotor height. The sprinklers that compose the spraying system are located at the very top of the room, 9 meters above the rotor and directly aligned with it so that the precipitation falls over the rotating blades during ice accretion. The spray ramp consists of 6 nozzles positioned in line to cover the entire width of the rotor from above. They operate in pulses by the electrical activation of a solenoid-driven piston that interrupts the flow of pressurized water periodically. This technology creates natural, controllable precipitation that provides great flexibility in precipitation conditions. The demineralized water comes from a pressurized refrigerated tank compressed at 80 psi. The main parameters affecting the MVD are the water pressure and the nozzle geometry.

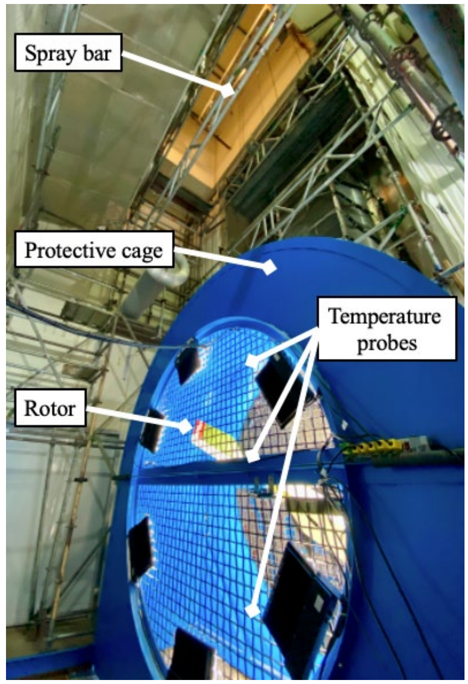

Figure **2.1.** Cold chamber disposition in CIIN's laboratory.

2.5.2 Droplet Size and MVD Measurement

The median volumetric diameter (MVD) is widely used to represent the droplet size distribution of a precipitation. It corresponds to the diameter at which 50% of the total volume of water in the size distribution is contained in droplets smaller than this diameter. By varying the water pressure and nozzle type, MVD of the droplets can be adjusted to the target value. In this study, the MVD was evaluated using microscopic photography of droplets collected on silicon oil-covered slides, based on the SAE AIR4906 [18].The measurement is performed in two phases. First, droplets are collected on the silicon oil-coated slides by passing the slides through the precipitation. Exposure time was kept very short to avoid droplet coalescence during collection and no significant spreading was observed during droplet measurement. Next, they are photographed under the microscope at 10X. For each slide, ten pictures like Figure 2.2 were taken, containing around 40 to 80 droplets each, resulting in more than 750 droplets sampled for each condition tested. Image processing is then employed to calculate droplet sizes from each image allowing to determine the MVD.

Figure **2.2**. Measurement method used to determine the mean volume diameter (MVD) of droplets.

2.5.3 Precipitation Intensity

The precipitation intensity is a useful parameter to characterize the intensity of ground icing events caused by larger droplet precipitations such as freezing rain. It measures the cumulated mass of water that falls on a specific area over a certain amount of time and is expressed in g/dm²/h. For the studied test bench, higher precipitation intensity leads to a greater rate of impact of the water droplets on the rotor and possibly faster ice growth. To accurately calibrate the precipitation intensity, a simple water collection method was employed, as used in other similar studies [19]. The sampling method is depicted in Figure 2.3 and based on the method described in standard SAE ARP5945 for deicing and anti-icing fluids [20]. Eight buckets are placed below the rotor, positioned linearly to cover the entire span of the rotor and swept area. During measurements, the rotor is static and placed vertically to avoid water collection disturbances. Over a period of 15 minutes for each tested combination of spray parameters, the collected water within each bucket is weighted to measure the mass collected over the time span. This allows for simple but effective characterization of the precipitation intensity and its spatial uniformity.

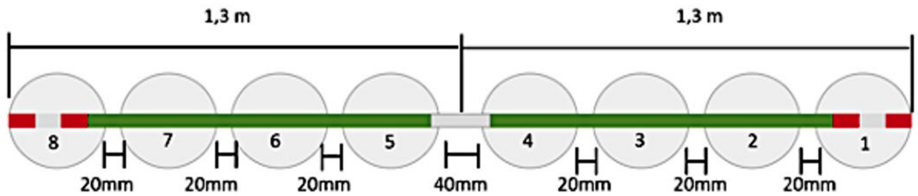

Figure **2.3**. Water collection method for precipitation intensity measurement.

2.5.4 LWC Calculation from Precipitation Intensity and MVD

The Liquid Water Content (LWC) is a key parameter in atmospheric icing which represents the mass of water contained per volume of air. Icing clouds and precipitations are characterized by their LWC and this parameter must usually be calibrated in simulated laboratory environments such as for the large-scale rotor test bench. Typically, the LWC is directly measured using a rotating cylinder method or a King Probe [21]. For this study, the parameter could not be directly measured with such instruments due to the lack of air velocity in the cold room, which is required for the proper functioning of such methods. However, the LWC can be calculated from the MVD and precipitation intensity measured experimentally [22]. The total mass of water droplets in a fixed volume of air can be approximated by measuring the mass of water collected over a defined area and time, assuming the droplets fall at a known velocity. The droplet velocity is determined by calculating the terminal velocity using the drag coefficient, which is in direct relation to the MVD. The study shows that for a 9 m fall, droplet MVD up to 1500 μm will reach terminal velocity, which encompasses the MVD conditions for wind turbine icing as presented in section 2.6. The terminal velocity of the droplets can be calculated with Equation 1 [22]. Then the measured precipitation rate can be directly converted to the corresponding LWC generated in the cold room using Equation 2 [22].

$$V_T = \sqrt{\frac{8}{3} r * \left(\frac{\rho_w}{\rho_{air}}\right) * \left(\frac{g}{C_D}\right)} \quad 1$$

$$LWC\left(\frac{g}{m^3}\right) = \frac{\lambda(g * m^{-2} * s^{-1})}{V_T(m * s^{-1})} \quad 2$$

2.5.5 Icing Conditions

Wind turbines experience a diverse array of icing events. These natural events are expressed using measurable parameters like air temperature, droplet MVD, LWC, etc. In order to obtain representative test conditions, the icing parameters used in this study are selected after investigating the conditions for moderate to severe freezing rain in the literature [23, 24]. The target MVD has been determined to be at 515 μm, which is representative of large droplets in freezing drizzle conditions, while the target LWC is 0.4 g/m^3, which corresponds to intense icing events [25, 26]. These conditions were validated by the icing data obtained from the research partners. One of these partners operate a small wind farm developed for research purposes and is fully equipped to characterize icing events. The icing conditions recorded at this wind farm over the last three years confirm that the selected conditions for this study correspond to a representative severe icing event affecting wind turbines during the winter period. It is important to note, however, that the icing conditions selected for this work represent only a small subset of the severe scenarios to which wind turbines may be exposed. The purpose of this study is not to study a complete icing envelope, but rather to demonstrate the capabilities of the newly developed test platform. Wind turbine icing events can happen under high humidity conditions and freezing temperatures close to 0°C which leads to aggressive glaze ice accretion, or under dryer, colder temperatures where a hard mixed ice will form [27]. In order to test ice protection systems for those two different types of ice (glaze and hard mixed), testing is performed at two temperatures of -5°C and -12°C. The resulting icing conditions for both testing temperatures in this study (-5ºC and -12ºC) are presented in Table 2.1.

To set the target LWC in the cold room, the corresponding precipitation intensity must first be calculated, as outlined in the previous section. The icing cloud is then calibrated to match this target intensity to achieve the desired LWC. For example, to obtain an LWC of 0.4 g/m³ with a droplet MVD of 515 µm, a precipitation rate of 31 g/dm²/h is required.

Table 2.1. Ice Accumulation Conditions.

LWC (g/m³)	MVD (µm)	Intensity (g/dm²h)	Glaze Ice Temperature (ºC)	Hard Mixed Ice Temperature (ºC)
0,4	515	31	-5	-12

2.5.6 Surface Characteristics

The blades used in this development project are service-retired rotorcraft tail rotor blades featuring a aluminum leading edge. As ice accretion did not extend into the painted regions beyond the metallic surface, only the leading edge was characterized.

The surface roughness was characterized by using an optical profilometer (Profilm3D, Filmetrics®, USA) which uses white light interferometry and is capable of measuring surface roughness up to 0.05 µm. Measurements were performed using a magnification of 50x at five randomly chosen locations along the leading edge over surface areas of 400 µm x 400 µm. The roughness is characterized by two roughness parameters: the maximum peak to valley height (Sa) and the arithmetic mean height (Sq). Together, these metrics offer a quantitative basis for comparing surface topographies and evaluating their potential impact on ice accretion and adhesion behavior. Measurement results are presented in Table 2.2 and an example of the profilometry output is shown in Figure 2.4. The results are consistent with a moderately rough surface, characteristic of a wear-affected metallic surface, rather than the smoother profile of a polished finish.

Table 2.2. 3D Profilometry Roughness Measurements on the Ice Accretion Substrate.

Measurement position	Sa (µm)	Sq (µm)
1	4.865	6.729
2	4.151	5.746
3	3.842	4.716
4	2.542	3.486
5	4.882	6.175
Average	4.056	5.370
Std. deviation	0.960	1.286

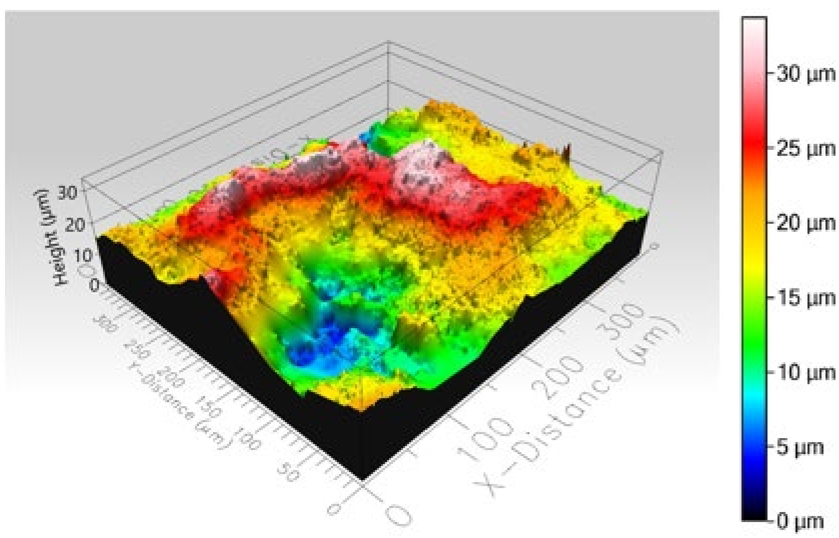

Figure 2.4. 3D Profilometry Roughness Measurements on the Ice Accretion Substrate.

The static water contact angle (WCA) was measured slightly aft of the leading edge on a slightly inclined region using a Drop Shape Analyzer DSA100E (Krüss GmbH, Germany), Figure 2.5.

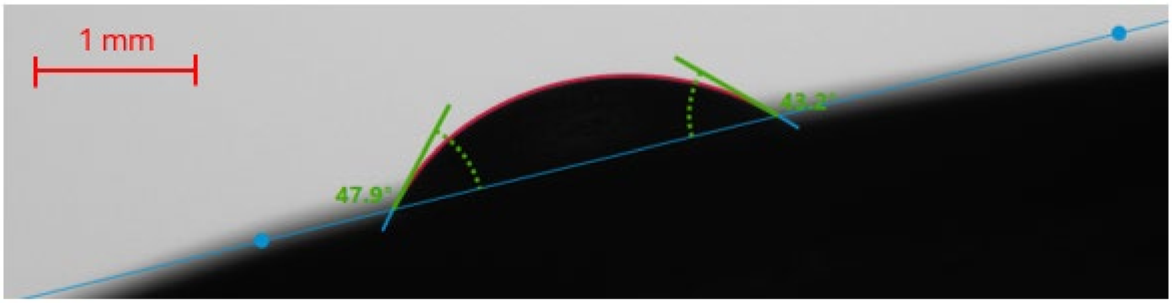

Figure 2.5. Static water contact angle on the aluminum substrate.

The static WCA was measured at different locations and an average of 43.6° as obtained. Due to the inclination of the surface, a slight difference in both angles measured from the profile was observed. The low contact angle indicates a high surface energy and hydrophilic surface which will favor good wettability during ice accretion and strong ice adhesion. This result is consistent with the surface roughness measurements indicating a relatively rough finish.

2.6 Materials and Methods: Large Scale Test Rotor Setup

2.6.1 Large Scale Rotor Assembly and Protection Cage

The experimental setup used in this study was originally developed to test deicing on a helicopter tail rotor. For the purpose of evaluating passive coatings for wind turbine blades, the helicopter tail rotor was used but at operating conditions matching wind turbines. One of the reasons the blades were not changed to test the adhesion of ice on wind turbine blades is because it allows for accurate representation of wind turbine blades tips, which are the most critical part in power production and the most susceptible to severe icing [7]. Most importantly, the centrifugal adhesion test at this scale requires rotational speeds that reach up to 1200 rpm and small-scale wind turbine blades that would fit this test bench are generally designed for a maximum rotational speed of 300 rpm which is not suitable for this application, hence the choice to keep the helicopter blades for this study. Moreover, matching substrate conditions at the ice interface between the ice and rotor blade is judged more critical than matching the complete structural configuration of life-size wind turbine blades.

The rotor itself has a diameter of 2.6 meters and is mounted on a direct-drive shaft out of a 100 hp three-phased asynchronous electrical motor. The rotor can be covered with a rolling cage, completing its protective enclosure to contain shattered ice and debris during the test, as shown in Figure 2.6. The refrigerated chamber and the test bench is equipped with vibration sensors, temperature probes at four different heights, surveillance cameras for test monitoring.

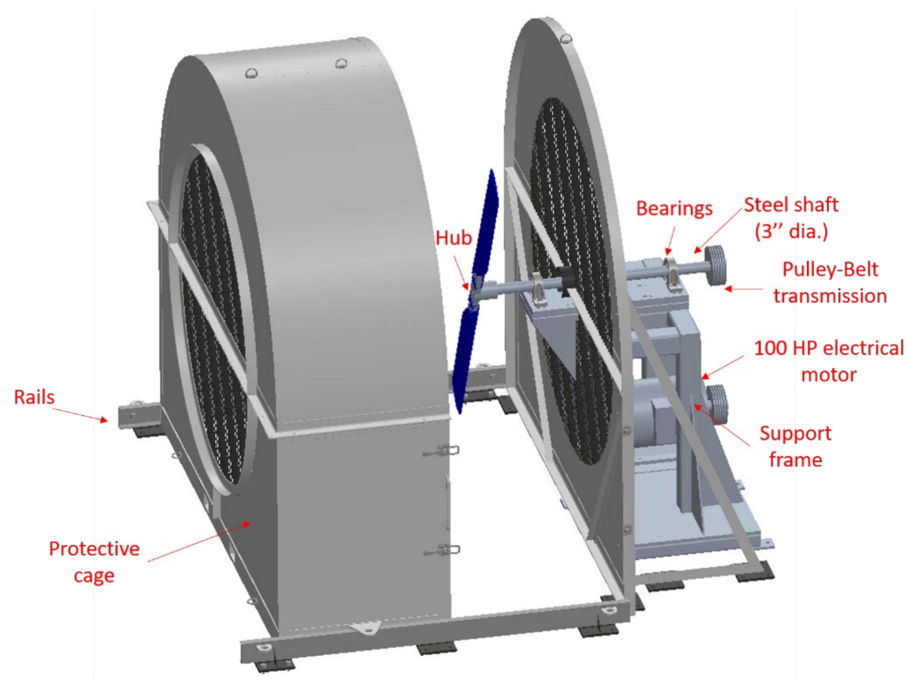

Figure 2.6. Diagram of the test bench inside the cooling chamber, the water spray ramp (not shown) is installed 9m above the rotor.

The precipitation conditions must be monitored precisely to achieve a representative ice accumulation, but this can only happen with the right speed of impact on the leading edge of the rotor, which is influenced by the rotational speed of the blades. During the accumulation phase, the protective cage needs to be rolled back to uncover the rotor. For safety reasons, the rotational speed is limited to 80 rpm during this phase to prevent the possibility of ice detaching. This rotational speed corresponds to approximately 40 km/h or 11 m/s. On the other hand, the rotor can reach 1200 rpm during the shedding phase which induces a maximal tip speed of 590 km/h or 163 m/s. These speeds are sufficient to replicate a wide range of icing and break-off scenarios that can occur on wind turbines in the field.

To monitor both the ice accumulation phase and the shedding part of the test, specialized cameras are the main tools used as they can help identify complex ice mechanics problems with visual confirmation. During the accumulation phase, a static picture of each blade is taken every three minutes, allowing to reconstruct a timelapse of the ice accumulation process of each blade

As for the shedding process, since the speed at which the event occurs is too fast to be captured normally, a Photron Fastcam Nova S6 high-speed camera recording at 6400 fps is used for this purpose. Pictures presenting this set up and an image of the produce slow-motion footage are presented in Figure 2.7. This tool is essential to the successful realization of the test since it can help to identify which blade out of the two is the first to shed ice. The second blade that sheds ice cannot be considered for data acquisition for the tests since its failure can most likely be triggered by the first blade’s detachment.

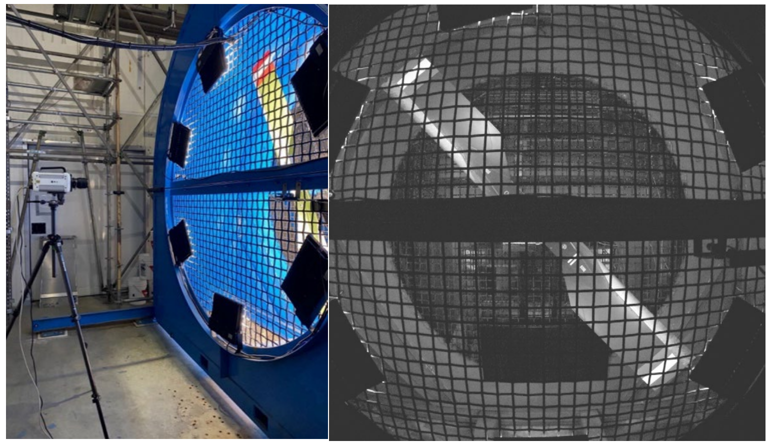

Figure 2.7. a) High-speed monitoring system. b) High-speed footage.

This overview presents the main equipment required for data acquisition and condition control for the research project. However, this test bench overview does not include the complex safety equipment required for the proper functioning of the test bench for sake of simplicity. Hence, it is important to keep in mind that safety measures are always active for every operation or test that is done on this large-scale test bench.

2.6.2 Ice Adhesion Strength Measurement

The test is designed in two separate phases: the accumulation of the ice layer on the blades and the shedding of ice from the blades. First, the ice accumulation phase focuses on building up a target amount of ice on the rotor blades. The rotor is exposed to freezing precipitation while spinning at 80 rpm. The amount of accumulated ice must allow ice shedding to occur before the limit rpm of 1200 is reached and this amount can be varied to test different scenarios and study the performance of passive ice protection systems. For the aluminum substrate used in this study, preliminary testing revealed that, under the test conditions selected for this study, the icing time should be approximatively 3,5 hours to obtain a total of 1 kg of ice per blade that will result in successful ice shedding in the second phase.

Once the ice accumulation is completed, the ballistic enclosure is closed around the rotor and the rotor is slowly accelerated until ice shedding is obtained. When the rotational speed is sufficiently high and the centrifugal forces exceed the sum of the adhesive and cohesive forces of the ice layer, ice shedding occurs. The forces acting on the ice are depicted in Figure 2.8 and expressed in Equation 3. To determine the adhesive shear strength, the methodology proposed by Fortin et Perron [28] is applied.

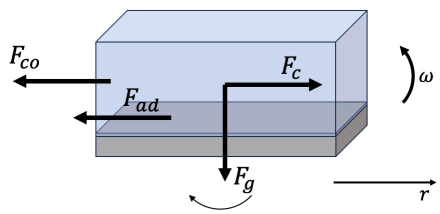

Figure 2.8. Free body diagram of infinitesimal block of ice on the rotor.

$$F_c = F_{co} + F_{ad} \qquad 3$$

Equation 3 assumes that the centrifugal force (F_c) acting on the center of mass of the block of ice is opposed by the cohesive and adhesive forces (F_{co}, F_{ad}). The gravitational force (F_g) is also acting on the ice in a rotating periodic manner as the rotor spins around its horizontal axis. However, this force is orders of magnitude smaller than the other forces at play, rendering it almost insignificant. The same reasoning applies to the bending and aerodynamic loads acting on the blades during rotation, which are therefore neglected.

With the data collected from the test, it is possible to evaluate the adhesive strength of the ice on the substrate, or maximal adhesive stress sustained, with Equation 4 [29]. This equation derived from Equation 3 calculates the adhesive strength of the ice τ_{ADH} (MPa) using the mass of the block of ice m_{ice} (kg), the radius of the center of the block of ice r_{ice} (mm), the cohesive strength of the ice σ_{COH} (MPa) measured and finally the cohesive A_{COH} and adhesive A_{ADH} areas of the detached ice at the rupture interface (mm^2). By measuring the surface area corresponding to the adhesive term, the shear stress at failure can be calculated. It is important to mention that complex failure mechanisms involving fracture mechanics are neglected in this study. The governing failure processes are considered to be influenced solely by the forces and stresses at play. Centrifugal adhesion testing is particularly useful in the case of large-scale atmospheric icing tests, as it allows the ice to be tested in its naturally accreted shape. This type of test also creates essentially no fractures in the ice before testing, which allows for accurate and repeatable results.

$$\tau_{ADH} = \frac{m_{ice} r_{ice} \omega^2 - \sigma_{COH} A_{COH}}{A_{ADH}} \tag{4}$$

2.6.3 Ice Cohesive Strength Measurement

As presented in the previous section, one of the parameters required to calculate the adhesive strength of the ice is its maximum cohesive stress. Literature shows that the cohesive strength of atmospheric ice varies significantly depending on the conditions and type of ice accreted [30]. Since the values of maximum cohesive stress vary widely according to the ice conditions and duration, basing this analysis on values from the literature can bring variability and inaccuracy in the results. Moreover, the maximum cohesive stress values presented in the literature itself varies greatly for similar icing event conditions. In order to obtain an accurate result for the adhesive strength, it is important to measure the cohesive strength of the accumulated ice layer with precision for both temperatures tested. To do so, another apparatus is installed next to the rotating blades during the ice accumulation process. The apparatus consists of rotating aluminum hollow cylinders which are placed in the same precipitation region as the rotor during the accretion phase as presented in Figure 2.9. The central portion of the cylinders consists of thin disks which are maintained together by a concentric tension rod during the ice accretion phase. After the ice accumulation, the tension rods are removed, and the cylinders are installed on a tensile test apparatus to measure the stress-deformation curve of the ice and the maximum cohesive stress obtained at failure of the ice. This method follows the procedure described by Harvey et al. in [31] and yields data specifically representative of the large-scale test bench, producing more accurate results. Every step of this testing procedure takes place in a controlled environment under the same conditions as the accretion phase.

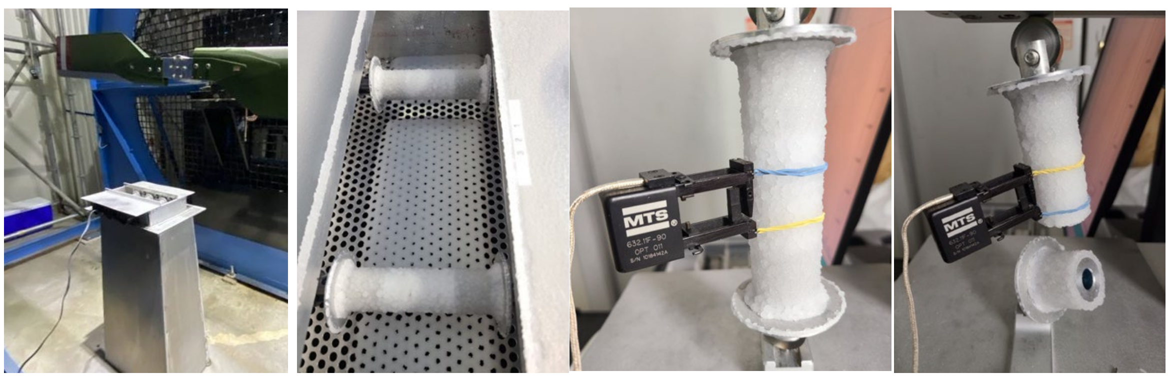

Figure 2.9. a, b) Cohesive strength evaluation setup with two rotating ice cylinders during accumulation. c, d) Ice cylinder before and after failure in the traction test apparatus.

2.6.4 Ice Shape and Surface Measurement (3D Scanning)

In order to accurately calculate the cohesive and adhesive forces and stresses, the corresponding surface areas on the blades must but measured with great precision after the ice shedding event. To accurately measure those surfaces, a three-dimensional optical volumetric scanner is used. A costume-built target grid, required for the scanner to position itself in space, was designed to fit specifically with the blade and ice geometry. This combination of tools allows to recreate a meshed numerical body of the blade and its ice shapes with a 0.2 mm volumetric accuracy. Figure 2.10 shows the highlighted adhesive surface on the blade after the break-off has occurred.

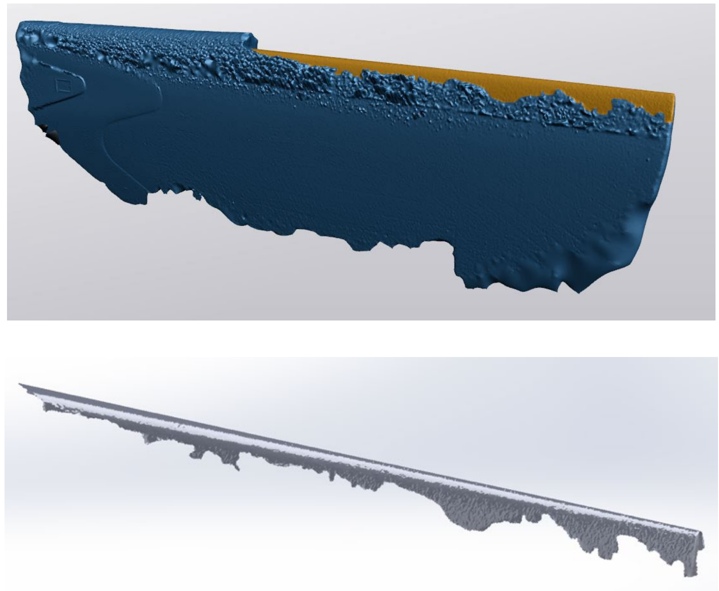

Figure 2.10.a) Numerical model of the blade after ice shedding. b) Corresponding adhesive area.

2.6.5 Ice Shedding Monitoring with High-Speed Imaging

High-speed imaging, as shown in section 3.1, is a crucial tool for the large-scale test bench, providing essential insights of the ice shedding process. Given the extremely fast nature of ice detachment, it is the most reliable method to determine which of the two blades sheds first, allowing for the adhesive strength calculation to be representative of the maximal internal stresses that occurred in the ice on the rotor blade. This is because after the shedding of the first blade, the rotor becomes unbalanced which increases significantly vibrations in the system, meaning that the second shedding may happen sooner than it would have if the only governing force was indeed the centrifugal force as intended. Additionally, high-speed footage, recorded at 6400 fps, enables the identification of fracture mechanisms by capturing the precise moments when cracks initiate and propagate, revealing key fracture points within the ice. This detailed visualization serves as a validation tool for experimental results, ensuring that observed adhesion behaviors align with theoretical predictions and contributing to a deeper understanding of ice-shedding dynamics.

2.6.6 Test Procedure

As proof of concept, this initial test campaign focusses on obtaining repeatable data and validating that the physical parameters of the tests are measured with sufficient precision. For this reason, these tests were conducted using aluminum blades mounted on the rotor of the test bench to avoid any effect of substrate aging, wear, and erosion on the ice adhesion measured. These results will serve as a low performance benchmark to be easily exceeded by carefully designed ice protection systems.

Each test requires a two-day period to include preparation and testing. The chamber is cooled to the targeted temperature at least 24 hours in advance to ensure that all the different and massive structures in the chamber have attained uniform temperature and no longer radiate heat which could influence the droplets temperature and solidification. The main components of the chamber and the blades are cleaned to remove any contaminants that could impact ice adhesion on the blades. The initial phase of testing is then initiated. The rotor is put in rotation at 80 rpm, and the sprinkler system is activated and continuously monitored for the duration of this phase to ensure that the conditions remain constant. The ice is gradually built up on the leading edges of the blades until the 3,5 hours accumulation period is over. Preliminary testing revealed that the ideal ice mass for centrifugal testing on the large scale to function properly is around 1 kg. This mass respects the limits imposed by the safety parameters for which the test bench was designed and is also sufficient to ensure shedding below the RPM limit of 1200 on the bare blades. Indeed, because of the blades' mass, ice mass should not exceed 1,5 kg to limit risks of structural failures during shedding and respect the limitation of the surrounding cage.

During this phase, the temperature of the chamber as well as the auxiliary cooling chamber are continuously monitored, and measures are taken every 30 minutes. The water pressure is also closely monitored to ensure that the projected droplets have a constant MVD. The goal of this phase is to keep the icing conditions as stable and conform to the target conditions as much as possible. At the end of the accumulation phase, the blades are weighted, the ice thickness is measured, and the blades are photographed as depicted in Figure 2.11.

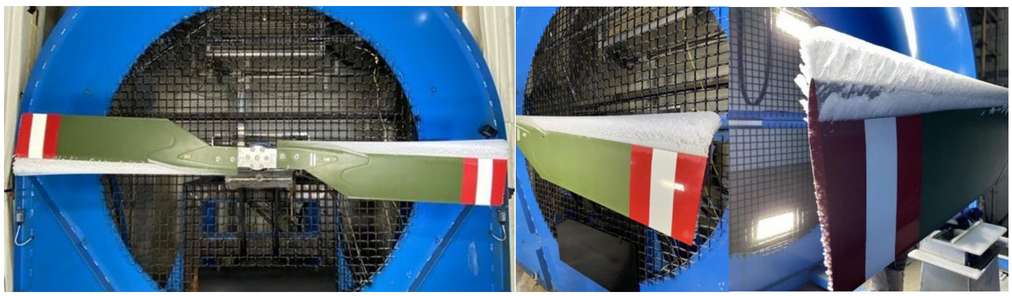

Figure 2.11. Hard mixed ice at -12ºC, a) Complete rotor. b) Single blade from the front. c) Single blade from behind.

The second phase of the test, the shedding, starts with the team securing the blades properly and closing the protective cage tightly. The monitoring equipment, the high-speed camera and the control center for the rotor drive are put in place. This test, contrary to the SRB test as seen in the literature review, unfolds as a constant-mass and varying-speed centrifugal adhesion test, meaning that the rotor is accelerated to slowly increase the centrifugal force applied on the ice but the mass does not change since there is no more accumulation at this point. The acceleration of the rotor is fixed at 7 rpm/s to avoid any dynamic phenomenon that could cause fragmentation in the rotor ice. When the rotational speed reached is high enough to cause delamination of the ice and a cohesive fracture closer down the radius of the blade, the separated block of ice contacts the cage at high speed. This impact triggers the cages and rotor shaft accelerometer threshold, cuts power to the motor drive and triggers the high-speed camera as shown in section 3.1. After the shedding, the rotor is safely brought to rest and it is possible to weight the blades after shedding, measure the length of ice detached and scan the surface area of the detachment and fracture zones on the blades, which correspond to the adhesive (A_{ADH}) and cohesive (A_{COH}) areas. Most of the time, the shedding tests on the large-scale test bench lead mixed fractures of the ice causing a partial detachment on the rotor blades as shown in Figure 2.12.

Figure 2.12. Fracture of the ice on rotor blade for hard mixed ice.

2.7 Results

2.7.1 Ice Cohesive Strength Evaluation

During this study on the development of the large-scale test bench targeted towards ice adhesion evaluation, ice cohesive stress evaluation was performed to obtain the cohesion of the ice accumulated on the rotor during the same precipitation conditions. The data acquired during the cohesive traction test includes the accumulated ice mass and thickness and the cohesive stress calculated at failure during the traction test as displayed in Table 2.3. The cohesive stress can then be calculated for each ice sample using the ratio of the maximal force applied over the cross-section area of the ice on the cylinder. The average stress-strain curves are generated for each ice type using the same data paired with the deformation data provided by the elongation probe placed on the samples. As shown in Figure 2.13, which presents the average data of every test's pair of cylinders, the brittle behavior of both types of ice can be observed as a sharp break in each curve.

Figure 2.13. a) Smoothed stress-strain curve at -12ºC of averaged two-cylinder tests. b) Smoothed stress-strain curve at -5ºC of averaged two-cylinder tests.

Table 2.3. Maximal and Average Cohesive Stress on Ice Cylinders.

Test	Target temp (°C)	Measured Temp (°C)	Cyl. 1 Cohesive Stress (MPa)	Cyl. 2 Cohesive Stress (MPa)	Cyl. Mean Coh Stress (MPa)	Mean Coh Stress (MPa)	Standard dev. (MPa)	Standard dev. (%)
1	-12	-13,45	1,13	1,29	1,21			
3	-12	-11,79	1,04	0,91	0,97			
4	-12	-12,16	1,86	2,00	1,93	**1,45**	0,37	25,40
5	-12	-12,13	1,43	1,68	1,56			
6	-12	-12,67	1,65	1,50	1,58			
7	-5	-4,95	1,10	1,30	1,20			
9	-5	-5,38	1,26	1,42	1,34			
10	-5	-5,14	1,23	1,24	1,24	**1,40**	0,22	15,57
11	-5	-5,18	1,74	1,70	1,72			
12	-5	-6,04	1,64	1,42	1,53			

The results show that a similar cohesive stress limit is obtained at -12ºC and -5ºC. The small difference between the two temperatures is insignificant compared to the standard deviations of the two data sets. Consequently, a mean cohesive stress value of 1,43 MPa shall be used to calculate the adhesive stress of the ice in both conditions. This mean value is in agreement with previous work on the same apparatus for similar conditions [31] and with a comparable research project carried out using a piezoelectric-based vibrating ice fracturing system [32]. Moreover, a review of the mechanical properties of ice done by Petrovic [33] showed that the tensile strength of ice normally ranges from 0,7 to 3,1 MPa with an average value of 1.43 MPa, [33] confirming the validity of the values obtained for the ice cohesive stress [30].

2.7.2 Ice Accumulation Results

The first step for each test is the ice accumulation phase. As explained under Section 3.6, accumulation is performed while the protection structure is pulled away from the rotor, and the blades rotate at a rotation speed of 80 RPM. The icing precipitation is then initiated and maintained for 3.5 hours to obtain 1 kg of ice on each blade. As shown in Table 2.4, the ice accumulation data for each test run includes ice thickness at the tip of the blade as well as the mass of ice accumulated on the entire blade. The data shows small variability in the results, at a similar level for both conditions, demonstrating the repeatability of the ice accumulation obtained with the test setup developed.

Table 2.4. Measured Temperature, Ice Thickness, and Ice Mass Accumulated on the Rotor Blades.

Target Temp (ºC)	Number of Tests	Avg. Temp. (ºC)	Avg. Tip Ice Thickness (mm)	Avg. Blade Ice Mass (kg)
-12	6	-12,2±0,4	53±3	0,96±0,08
-5	6	-5,1±0,3	46±1	0,88±0,07

The data reveals slight differences in the ice accumulation obtained between the two icing temperatures tested. First, the average mass obtained at –5ºC is slightly lower than the one at -12ºC for the same accumulation time. At the warmer temperature, it is not all the droplets that freeze at impact, allowing some droplets to flow off the blade which results in a slightly smaller mass accumulated, which is in line with the changing ice type. Indeed, at the colder temperature of -12ºC a dense mixed, near rime, ice is obtained compared to the denser glaze accumulation obtained at –5C, as seen on Figure 2.14. This also explains the higher average ice thickness than for the warmer temperature of -5ºC, with an average value at 53 mm, 17% thicker than at -5ºC. This result is common in literature where rime ice is usually obtained at colder temperatures while glaze ice is obtained at warmer temperature closer to the freezing point.

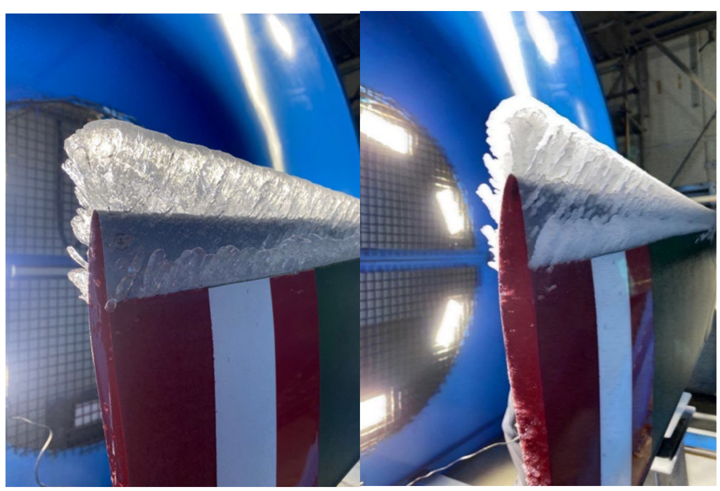

Figure 2.14. Difference in ice types under the two icing conditions, a) -5ºC. b) -12ºC.

In both cases, the ice formation tends towards the same shape built of small, towering agglomerates stacked close to one another. Closer to the leading edge, these structures merge completely with each other and form a solid block of ice, similar to what can be observed on actual wind turbine blades in the field during severe icing events and comparable to an ice formation study on small scale wind turbines [10, 34].

2.7.3 Ice Adhesive Stress Evaluation

One of the primary objectives of the large-scale test setup is to allow the evaluation of ice adhesion and shedding characteristics from different substrates across multiple representative atmospheric conditions. To validate the developed test rig and associated methodology, a total of 12 tests were conducted, with 6 tests at -12°C and 6 tests at -5°C, on the bare aluminum blades. After the ice accumulation process, presented in the previous section, the second step for each of those tests was to obtain ice shedding to measure the adhesion of the ice on the substrate. The blade rotation speed was gradually increased at a rate of 7 rpm/s until ice shedding occurred. With the high-speed imaging, it was then possible to monitor from which blade the ice detached first. Then the mass and length of ice shed from that blade was measured for the ice adhesive strength calculation. The surface of the blade exposed after the ice shedding as well as the surface of the ice break was measured using the numerical scanner. The adhesive stress is calculated with the collected data using the centrifugal adhesion test equation and the results are collected in Table 2.5.

Table 2.5. Centrifugal Adhesion Test Data and Maximal Calculated Adhesive Stress on Bare Aluminum Rotor Blades.

Target Temp. (ºC)	#	Measured Temp (ºC)	Shed Ice Mass (kg)	Shed Ice Length (mm)	RPM_{max}	COH Stress (MPa)	ADH Stress (MPa)	Avg. ADH Stress (MPa)	Std. Deviation (MPa)	Std. Deviation (%)
-12	1	-11,6	0,44	390	796	1,43	0,25	**0,25**	0,04	15
	2	-11,0	0,46	360	828		0,24			
	3	-12,5	0,41	320	757		0,18			
	4	-12,2	0,56	380	840		0,24			
	5	-12,1	0,62	394	808		0,28			
	6	-12,7	0,45	330	819		0,29			
-5	7	-4,9	0,37	320	816	1,43	0,22	**0,16**	0,06	36
	8	-5,0	0,45	360	664		0,13			
	9	-4,7	0,39	330	618		0,06			
	10	-5,4	0,4	289	644		0,15			
	11	-5,3	0,54	430	645		0,19			
	12	-5,1	0,31	272	693		0,17			

The average maximum adhesive stress measured is approximately 0,25 ± 0,04 MPa for -12°C and is 0,16 ± 0,06 MPa in the case of -5°C with respective standard deviations of 15% and 36%. The values obtained are aligned with the expected results as theory suggests that atmospheric ice in conditions closer to the freezing point should be less adherent to the substrate on which it is formed. This 0,09 MPa difference can be explained by the increased importance of the liquid-like layer at the borders of the crystal structure of the ice accumulated on the blades of the rotor. These layers lack structure and can encourage slipping of the ice, especially in conditions closer to freezing point where thermal energy is higher. This difference in failure mode was consistently observed, as shown in Figure 2.15, with the colder condition leading to a cleaner and more linear detachment due to grouped ice shedding.

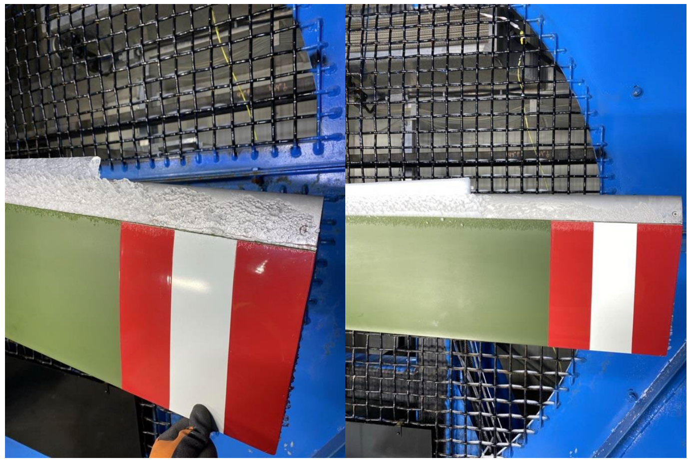

Figure 2.15. a) Shedding of the ice at -5ºC on aluminum blades. b) Shedding of the ice at-12ºC on aluminum blades.

As reported in the literature, the adhesion strength of ice tends to decrease near the freezing point, where glaze ice forms, and increases as the temperature drops and the ice transitions into harder mixed ice. However, if the temperature were lowered further, the adhesion strength would likely decrease again, as cold rime ice loses structural integrity and becomes more fragile [35]. The shear strength values obtained with the large-scale test rig are within the range of values measured with similar test benches found in the literature. First, the Spinning Rotor Blade test bench (SRB), despite its smaller scale obtained an adhesion value for ice on aluminum of 0,11 ± 0,04 MPa at -5ºC and of 0,21 ± 0,06 MPa at -15°C [11, 29]. The AERTS, another similar setup with a similar scale but with a vertical rotation axis, measured adhesion values of ice on aluminum with different surface roughness to be between 0,157 MPa at -8ºC and 0,293 MPa at -16ºC [36], very similar to the value obtained in this study. Both cases show that the values presented within the current work are coherent and reliable. Additionally, it is possible to observe that the adhesive strength at warmer conditions presents more variability, as highlighted by Figure 2.16.

Figure 2.16. Adhesive stress at failure measured for ice accreted on bare aluminum rotor blades.

The length and mass of shed ice during the test are valuable metrics for future comparison with passive ice protection systems once the test bench is applied to coating evaluations. As presented in Table **2.5**, these metrics proved to be relatively consistent within each temperature condition, with average shedding masses of approximately 0.49 kg and shedding lengths of 362 mm at –12 °C, and 0.41 kg and 334 mm at –5 °C. This consistency suggests good repeatability of the test procedure, even though the initial accumulated ice mass varied between trials. When assessing the performance of surface coatings designed to reduce ice adhesion, such coatings may trigger shedding at lower rotational speeds but over shorter ice segments. This behavior could significantly influence the interpretation of results and offer insight into the mechanical response of the ice–surface interface. Monitoring these parameters alongside adhesion stress could help characterize not only the effectiveness and performance of icephobic coatings, but also their influence on shedding dynamics, such as crack propagation and failure modes.

The characterization of ice failure modes represents one of the primary avenues for future development using this test bench. However, capturing fracture initiation and propagation on a large-scale rotating system requires extremely high temporal and spatial resolution across the entire rotor radius, capabilities that currently limit the ability of this setup to draw firm conclusions about the governing detachment mechanisms in the present dataset. Future work incorporating enhanced high-speed imaging and expanded testing campaigns will enable a more detailed investigation of these processes. Advancing ice shedding prediction models, supported by large-scale experimental data from this new test bench, constitutes a key research direction for the continued development of atmospheric icing mitigation strategies.

2.8 Conclusion

This study presents the development and validation of a novel large-scale horizontal-axis rotor test bench designed to simulate representative freezing rain conditions of wind turbine environments. Key atmospheric ground icing parameters, such as temperature, median droplet size, and liquid water content, are accurately reproduced in a large cold chamber, enabling controlled ice accretion on a large-scale test rig. The test rig allows to recreate representative centrifugal ice shedding scenarios on rotating blades. The test conditions selected for this new test rig were based on the literature and on in-field measurements performed by the research partner on their wind turbines during icing events.

The unique sequence of accumulation, pause, and shedding phases allows for precise characterization of both ice geometry and properties before its detachment used for adhesion characterization. Proof of concept testing was then performed on the bare aluminum blades to validate the test rig. This first data, for the validation of this innovative test bench, serve as a reference for future test campaigns on other substrates. The measured adhesive stresses on bare aluminum blades averaged 0.24 ± 0.05 MPa at -12 °C and 0.17 ± 0.06 MPa at -5 °C, in close agreement with reported atmospheric ice adhesion values from other smaller scale tests in the literature. Moreover, the cohesive stress evaluation resulted in a value of 1.43MPa which also aligns properly with the findings of similar studies. Despite natural variability in atmospheric ice formation, the repeatability of the rig was also demonstrated by the low standard deviations obtained, especially for the accumulation phase, reinforcing the reliability of the rig and test procedure.

The validated test rig will allow new research studies to be initiated. First, it will allow the evaluation of specifically engineered ice adhesion reduction coatings. These materials are designed for passive ice protection on wind turbines and will be assessed under identical conditions to quantify their performance and durability. The test bench will also open the possibility of investigating hybrid protection systems and in-cloud icing scenarios. Its large scale, environmental control, and precision measurement capabilities position it as a unique platform to advance the field of atmospheric icing research and support the development of more resilient wind energy technologies. Finally, the test rig will also be used to perform fundamental studies of the mechanisms involved in ice shedding and fracture to better understand ice properties.

2.9 Acknowledgement

The financial and scientific support from AMIL, NSERC, FRQNT, IDEaS, Nergica and Mont-Sainte-Marguerite Wind Farm is kindly acknowledged. The authors thank essential team members Patrice Rondeau, Luc Chatigny and Carol Mercier for their essential work.

2.10 References

1. Afzal, F. and M.S. Virk. Review of icing effects on wind turbine in cold regions. in E3S web of conferences. 2018. EDP Sciences.

2. Icing loss Data from Mont-Sainte-Marguerite Wind Farm, in Project Kick-Off Meeting, P. Energy, Editor. 2023.

3. Fortin, G., Simulation de l'accrétion de glace sur un obstacle bidimensionnel par la méthode des bissectrices et par la modélisation des ruisselets et des gouttes de surface. 2003: Université du Québec à Chicoutimi.

4. Lamraoui, F., et al., Atmospheric icing impact on wind turbine production. Cold Regions Science and Technology, 2014. 100: p. 36-49.

5. Fakorede, O., et al., Ice protection systems for wind turbines in cold climate: characteristics, comparisons and analysis. Renewable and Sustainable Energy Reviews, 2016. 65: p. 662-675.

6. Parent, O. and A. Ilinca, Anti-icing and de-icing techniques for wind turbines: Critical review. Cold regions science and technology, 2011. 65(1): p. 88-96.

7. Hochart, C., et al., Wind turbine performance under icing conditions. Wind Energy: An International Journal for Progress and Applications in Wind Power Conversion Technology, 2008. 11(4): p. 319-333.

8. Mayer, C., et al., Wind tunnel study of electro-thermal de-icing of wind turbine blades. International Journal of Offshore and Polar Engineering, 2007. 17(03).

9. Minoofar, G., et al., Progress in Icephobic Coatings for Wind Turbine Protection: Merging Chemical Innovation with Practical Implementation. Crystals, 2025. 15(2): p. 139.

10. Drapalik, M., L. Zajicek, and S. Purker, Ice aggregation and ice throw from small wind turbines. Cold Regions Science and Technology, 2021. 192: p. 103399.

11. Villeneuve, E., C. Blackburn, and C. Volat, Design and development of an experimental setup of electrically powered spinning rotor blades in icing wind tunnel and

preliminary testing with surface coatings as hybrid protection solution. Aerospace, 2021. 8(4): p. 98.

12. Shu, L., et al., Numerical and experimental investigation of threshold de-icing heat flux of wind turbine. Journal of Wind Engineering and Industrial Aerodynamics, 2018. 174: p. 296-302.

13. Work, A. and Y. Lian, A critical review of the measurement of ice adhesion to solid substrates. Progress in Aerospace Sciences, 2018. 98: p. 1-26.

14. Andrews, E. and N. Lockington, The cohesive and adhesive strength of ice. Journal of materials science, 1983. 18: p. 1455-1465.

15. Han, Y., J. Palacios, and S. Schmitz, Scaled ice accretion experiments on a rotating wind turbine blade. Journal of Wind Engineering and Industrial Aerodynamics, 2012. 109: p. 55-67.

16. Lübker, J., et al., DLR Whirl Tower Icing & De-Icing Facility. 2022.

17. Fortin, G. and J. Perron. Wind turbine icing and de-icing. in 47th AIAA Aerospace Sciences Meeting including The New Horizons Forum and Aerospace Exposition. 2009.

18. SAE, SAE International AIR4906. Droplet Size Instrumentation Used in Icing Facilities. 1995, SAE International: Warrendale, PA, USA.

19. Orchard, D., Investigation of tolerance for icing of UAV rotors/propellers: Phase 3 test results. Laboratory Memorandum (National Research Council of Canada. Aerospace. Aerodynamics Laboratory); no. LM-AL-2021-0051, 2021.

20. SAE, ARP5945 Endurance Time Tests for Aircraft Deicing/Anti-icing Fluids SAE Type I. 2016.

21. SAE, Aerospace Standard ARP5905. Calibration and Acceptance of Icing Wind Tunnels. 2003, AC-9C Aircraft Icing Technology Committee: Warrendale, PA, USA.

22. Villeneuve, E., et al., An experimental apparatus for icing tests of low altitude hovering drones. Drones, 2022. 6(3): p. 68.

23. Jolin, N., et al., Wind turbine blade ice accretion: A correlation with nacelle ice accretion. Cold Regions Science and Technology, 2019. 157: p. 235-241.

24. SAE, ARP5485B - Endurance Time Test Procedures for SAE Type II/III/IV

Aircraft Deicing/Anti-Icing Fluids. 2017: SAE International.

25. Xu, Z., et al., A parametric study on the effect of liquid water content and droplet median volume diameter on the ice distribution and anti-icing heat estimation of a wind turbine airfoil. Results in Engineering, 2024. 22: p. 102121.

26. Battisti, L., Wind turbines in cold climates: Icing impacts and mitigation systems. 2015: Springer.

27. Godreau, C., et al., Definition of Best Practice for Testing Icephobic Surfaces. 2022.

28. Fortin, G., A. Beisswenger, and J. Perron. Centrifuge adhesion test to evaluate icephobic coatings. in AIAA Atmospheric and Space Environments Conference. 2010.

29. Fortin, G. and J. Perron. Spinning rotor blade tests in icing wind tunnel. in 1st AIAA Atmospheric and Space Environments Conference. 2009.

30. Palanque, V., et al., Cohesive strength and fracture toughness of atmospheric ice. Cold Regions Science and Technology, 2022. 204: p. 103679.

31. Derek Harvey, G.M. Development of a Test Apparatus for the Measurement of Tensile Properties of Accreted Ice. in International Workshop on Atmospheric Icing of Structures (IWAIS). 2024. Narvik.

32. Villeneuve, E., C. Volat, and S. Ghinet, Numerical and Experimental Investigation of the Design of a Piezoelectric De-Icing System for Small Rotorcraft Part 3/3: Numerical Model and Experimental Validation of Vibration-Based De-Icing of a Flat Plate Structure. Aerospace, 2020. 7(5): p. 54.

33. Petrovic, J., Review mechanical properties of ice and snow. Journal of materials science, 2003. 38: p. 1-6.

34. Kraj, A.G. and E.L. Bibeau, Phases of icing on wind turbine blades characterized by ice accumulation. Renewable Energy, 2010. 35(5): p. 966-972.

35. Guerin, F., et al., Analytical model based on experimental data of centrifuge ice adhesion tests with different substrates. Cold Regions Science and Technology, 2016. 121: p. 93-99.

36. Smith Jr, J.G., et al., Impact ice adhesion strength of stainless steel 304 as determined on a centrifuge test stand. Cold Regions Science and Technology, 2022. 196: p. 103492.

2.11 Major Contributions

In this paper, Thomas Allard, supported by Éric Villeneuve, Derek Harvey, Patrice Rondeau and Luc Chatigny, primarily worked on the design and execution of the experimental procedure from the characterization of the target conditions in the test bench's chamber to the finalization of the data collection for ice adhesion. Gelareh Momen aided in interpreting the results and drafting the manuscript. The redaction of the manuscript was carried out by Thomas Allard and Éric Villeneuve.

CHAPTER 3

From Lab to Blade: Scalable Validation of a Durable Silicone-Epoxy Icephobic Coating for Wind Turbine Blades

3.1 Paper Presentation

This second article investigates the performance of a commercial silicone–epoxy icephobic coating for wind turbine blades using a multi-scale experimental comparison. It addresses the lack of large-scale validation commonly found in studies on passive ice protection methods. The scientific contribution of this work lies in linking standard laboratory characterization with realistic large scale rotor adhesion tests. The coating is first characterized following ISO/TS 19392 standards, confirming its durability and low ice adhesion over repeated icing/de-icing cycles. Ice adhesion and shedding behavior are then evaluated using push-off, CAT, spinning rotor blade, and finally large-scale tests.

A key outcome of this study is the identification of scale-dependent ice detachment mechanisms. While laboratory scale tests predominantly show adhesion-driven failure, large-scale rotating tests more often result in cohesive and adhesive, or mixed, failures of the accreted ice. This demonstrates how laboratory measurements can be used to predict expected trends and limitations of coating performance under operational conditions.

This article corresponds to the second phase of this master's research project, which focuses on applying the developed large-scale test methodology to evaluate passive icing protection systems. It validates the reliability and scalability of the centrifugal adhesion test approach and provides practical insight into how passive coatings may contribute to ice mitigation on wind turbines.

This article constitutes a continuation of the first published paper and was published in the journal *Engineering Structures* (Elsevier) on January 20th 2026. This work aligns with one of the main objectives of the thesis by comparing the performance evaluations methods at different scales for passive icing protection coatings. Hence, it substantiates the potential of these test methods for real industrial applications in this field of research.

3.2 Paper Manuscript

From Lab to Blade: Scalable Validation of a Durable Silicone-Epoxy Icephobic Coating for Wind Turbine Blades

Authors: Ghazal Minoofar[1], Gelareh Momen[1,2], Thomas Allard[1], Derek Harvey[1], Éric Villeneuve[3] and Reza Jafari[1].

Affiliations: [1]Department of Applied Sciences, University of Québec in Chicoutimi, [2]École de technologies supérieures, [3]Département de mathématiques, informatique et génie de l'Université du Québec à Rimouski.

Corresponding author: Gelareh Momen.

REVISION 1

3.3 Abstract

Ice accumulation on large rotor blades poses a major operational challenge by reducing energy output and threatening structural integrity. Active de-icing systems are effective but limited by high energy demand, delayed response, and elevated costs. Passive solutions, particularly silicone–epoxy icephobic coatings, offer advantages such as low surface energy, durability, and reduced ice adhesion, enabling earlier shedding. However, most studies remain confined to laboratory scale without validation under realistic conditions.

This study addresses this gap by evaluating a durable commercial silicone–epoxy coating at both laboratory and large scales. Laboratory characterization following ISO/TS 19392 standards showed a water contact angle of 100° ± 2.2°, mechanical abrasion resistance of 72 ± 2.1 mg/1000, and ice adhesion strength below 20 kPa even after 50 icing/de-icing cycles, confirming strong icephobic performance. Push-off and CAT tests with short ice specimens predominantly exhibited adhesion-dominated detachment, favorable for anti-icing. In contrast, spinning rotor blade and field trials with more realistic accretions often resulted in cohesive or mixed failures, leaving residual ice. These results indicate that adhesion-focused behavior observed in small-scale tests correlates with the more complex detachment dynamics at larger scales, demonstrating how laboratory measurements can predict expected performance and benefits under operational conditions.

Overall, the study demonstrates the value of integrating quantitative material properties with multi-scale adhesion testing to guide the design of ice-mitigation coatings, as pictured in Figure 3.1. In practice, the coating's role is best understood as part of broader ice protection strategies, where variables such as rotation speed during accretion strongly influence shedding.

Keywords: Wind-turbine Anti-icing, Passive Methods, Icephobic Surface Coatings, Large-scale Performance Evaluation, silicone-epoxy coating

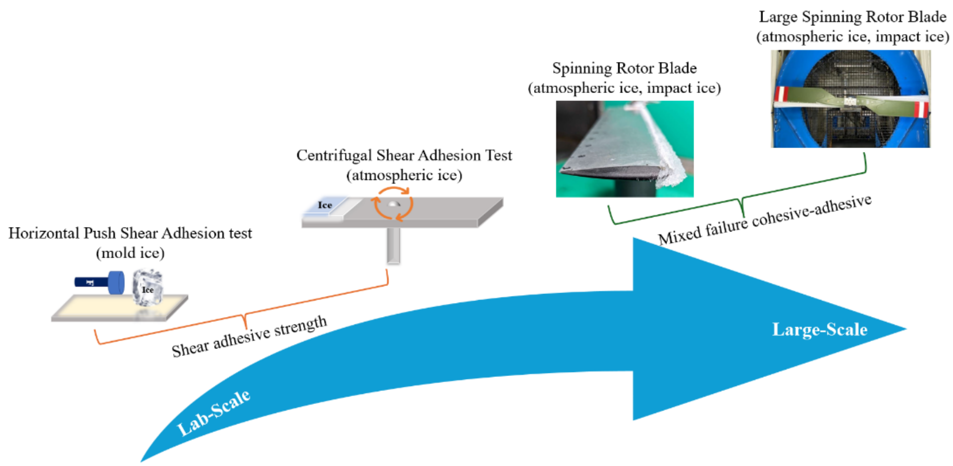

Figure 3.1 Scaling of Ice Adhesion Test Methods

3.4 Introduction

The growing demand for renewable energy has established wind turbines as essential components in the global shift towards sustainable power sources [1]. the performance of wind turbines improves as the temperature decreases [2,3], however, a significant challenge these turbines face is the accumulation of ice on their blades, which can severely hinder aerodynamic performance, reduce energy efficiency, and compromise operational reliability [4,6]. While several active anti-icing methods, such as electro-thermal heating, hot air circulation, and mechanical de-icing systems, have been designed and employed to address this issue, they often suffer from high energy consumption, increased operational complexity, and maintenance demands, especially under harsh environmental conditions [5,7,8]. To mitigate this issue, the advancement of anti-icing coatings has become a key focus in addressing ice accumulation on wind turbine blades due to zero emission benefits, operational costs and energy usage. To be effective, anti-icing coatings designed for wind turbines need to satisfy several critical performance requirements [9,10]. Mechanical robustness is essential, as the coatings must endure environmental and operational stresses, including wind-induced forces, blade elongation, and bending. Standards such as ISO 527-1, ASTM D2240, and ASTM D4060 are commonly used to evaluate tensile strength, hardness, and abrasion resistance, respectively, ensuring the durability of coatings under such conditions [11,13]. In addition to mechanical performance, these coatings must exhibit high icephobicity to minimize ice accumulation and adhesion, critical for maintaining aerodynamic efficiency and reducing maintenance needs. This is assessed according to ISO/TS 19392-6:2023, which provides testing guidelines for icephobic properties in wind turbine applications [14]. Rain erosion resistance is another critical factor; coatings need to withstand impacts from water droplets that can strike blade tips at speeds nearing 90 m/s on large wind turbines (ISO/TS 19392-3) [15]. Additionally, abrasion resistance is essential for maintaining performance under harsh environmental conditions [16]. These characteristics are largely determined by the polymer selected as the base resin [17,19]. Among polymer-based resins, silicone-epoxy coatings stand out for their superior performance, particularly in harsh environmental conditions, due to the synergistic combination of the unique properties of both silicone and epoxy. The silicone component imparts low surface energy to the coating, which plays a crucial role in reducing ice adhesion strength (τice) by weakening bonding forces between the ice and the surface [20]. This also contributes to low wettability, minimizing water accumulation and promoting droplet roll-off, factors that further enhance icephobic behavior. Meanwhile, the epoxy component provides mechanical robustness, strong adhesion to various substrates, and resistance to wear and environmental degradation

[21], resulting in coatings that are not only durable but also highly icephobic. As a result, silicone-epoxy coatings are especially interesting for applications where resistance to ice accumulation and ease of ice removal are essential for maintaining operational reliability in subzero environments [22,23]. However, despite their promising potential, these coatings face challenges such as limited large-scale validation, susceptibility to mechanical damage under harsh icing conditions, and potential degradation over long-term field exposure. Consequently, studies on the anti-icing performance of silicone-epoxy coatings remain relatively few, with development efforts concentrated in a small number of research groups [24,26]. Typically, these researchers employ a range of methodologies to enhance the icephobic properties of silicone-epoxy resins, as detailed below. For example, Momen et al. [27] recently fabricated an icephobic silicone–epoxy hybrid coating using commercial silicone–epoxy resins (SILIKOPON® EF & ED), two fluorinated silicone additives, and amino-functional silane-curing agents for steel substrates. They reported an τice for 94kPa. Further research [28] examined the anti-/de-Icing performance of epoxy coatings with GO-PPy@SiO2 as photothermal fillers. The researchers claimed that at an optimal filler concentration, the water droplet on their produced coating remained unfrozen for 710 seconds at -15°C, effectively delaying icing. Also, when their sample was exposed to simulated sunlight, the surface temperature of the coating rapidly increased from room temperature to over 80 °C within 10 minutes, peaking at 84.9°C, resulting in frozen droplets melting within just 5 seconds. Ziętkowska et al. [29] tailored a commercial silicone-epoxy resin (SILIKOPON® ED) through the incorporation of dually functionalized polysiloxanes to fabricate icephobic coatings for photovoltaic panel utilizations. They found that the chemical modification significantly improved the icephobicity of the prepared coatings with a 69% decrease τice (reaching below 100 kPa) and 17 times increase in the freezing delay time in

comparison with the pure ones. The silicon-epoxy coatings showed a CAH of 7° to 11° and a roll-off angle of 32° to 55°. Following the approach of Zhao et al. [30] a robust icephobic coating was developed using an interpenetrating polymer network (IPN) of epoxy and PDMS. Low-molecular-weight silicone oil was also incorporated to reduce the crosslink density, allowing precise control of the coating's elastic modulus. This adjustment contributed to achieving optimal icephobic properties by balancing low ice adhesion and coating strength. Testing demonstrated that the coating's τice reached approximately 8 kPa at an elastic modulus of 0.18 MPa. Even after 25 cycles of icing and de-icing, the coating remained stable, with τice consistently maintained between 3 and 14 kPa. In another study, Sullivan et al. [31] designed a dual-function anti-icing system featuring a superhydrophobic layer supported by an embedded thin-film heating element. After 52 seconds heating, the SiO_2-PDMS coating exhibited rapid thermal response up to 60 °C. It also showed superhydrophobicity with a 164° contact angle and 3° hysteresis. In cold chamber tests, the hybrid coating reduced ice adhesion by 83% (from 284 kPa to 50 kPa) and delayed freezing, achieving full anti-icing with 0.34 W/cm^2 power density, reducing energy consumption by 37%. Zhang et al. [32] fabricated a durable, anti-corrosive superhydrophobic coating with photothermal properties, made with Fe3O4 composite nanoparticles in dual sizes (200nm and 20 nm) for anti-icing and de-icing applications, which was sprayed onto glass substrates. The coating,), PDMS as a protective layer, and epoxy as the basecoat, uses Fe3O4 NPs optimized to achieve superior micro/nanostructures. This design enhances photothermal conversion under simulated sunlight with a radiation intensity of 1 kW/m^2, achieving a heating rate of 14.4 °C/min and a light-to-heat conversion efficiency of 62.38%. [33].

Despite extensive research on various icephobic materials, a significant gap remains in translating laboratory findings into real-world applications, particularly for wind turbine blades exposed to dynamic, harsh, and variable environmental conditions [34,35]. Most studies have been limited to small-scale tests [36] on flat, idealized surfaces under simplified icing conditions, often leading to complete ice detachment due to short interface lengths and purely adhesive failure modes, where the bond between the ice and the substrate fails at the ice/substrate interface [37,38]. However, real-world ice accretion involves both adhesive and cohesive failures across much longer spans [39,40]. In operational turbines, ice buildup reduces rotational speed (RPM), diminishing the centrifugal forces essential for passive ice shedding, especially against dense ice types like glaze or hard rime, where gravity or aerodynamic forces are typically insufficient. While full-span shedding is ideal, the outer third of the blade is particularly critical, as it contributes most to lift and energy output. Low τice measured in the lab can support passive shedding by allowing centrifugal and aerodynamic forces to remove ice more easily, potentially improving energy production, reducing downtime, and lowering maintenance costs—though its effectiveness depends heavily on in-field conditions. This study aims to bridge this lab-to-field gap by evaluating a commercially available silicone-epoxy coating (Lotus Dry) from our industrial partner, Techeol, Canada, under realistic geometries, ice types, and mechanical stresses to assess its practical ice-shedding performance on wind turbine blades.

The study is structured in two phases: the first phase involved detailed laboratory characterization of the silicone-epoxy coating, with various tests conducted to assess their icephobic, mechanical and durability properties. The second phase transitioned from small-scale laboratory characterization to larger scale realistic testing by applying the coatings on

1.3 m radius x 2.6 m long rotor blades installed in a 12 m high cold room, to evaluate their performance under simulated atmospheric icing conditions. This approach takes into account environmental factors such as droplet size, liquid water content, wind speed, and precipitation intensity, providing a comprehensive understanding of the coatings' effectiveness in mitigating ice accumulation on wind turbines.

This dual-scale investigation, by examining both laboratory characterization and large-scale applications, offers a deeper understanding of how these coatings can be optimized to address the challenges faced by wind turbines in cold climates, while also demonstrating the correlation between lab-scale and larger-scale more representative tests, ultimately contributing to improved performance and energy efficiency.

3.5 Materials and Methods

3.5.1 Material

The commercial silicone-epoxy coating (Lotus Dry), used as the primary topcoat in this study, was obtained from Techeol, Canada. This coating was selected for its advertised hydrophobicity and weather resistance, highlighting its potential as a candidate for improving the surface durability under harsh environmental conditions. As the base layer and reference for comparative analysis, a polyester gel coat (VIBRIN G290AA) supplied by AOC was applied. This specific gel coat was chosen because it is commonly used in industry as a protective layer on fiberglass-epoxy composite wind turbine blades. Its established performance and compatibility with composite substrates make it an ideal benchmark for evaluating the enhancements offered by the silicone-epoxy topcoat.

3.5.2 Sample Preparation

In this study, specimen preparation methods were tailored to the specific requirements of each test, considering variations in geometry, surface conditions, and coating application. Detailed preparation procedures are provided in the respective sections corresponding to each test. All aluminium substrates used were first cleaned with acetone to remove surface contaminants and then pre-coated with a polyester gelcoat (VIBRIN G290AA). Aluminum is widely used in aerospace, and other engineering components. Testing on aluminum provides results that are closer to what would be expected in real-world applications. Gelcoat layer was allowed to fully cure at room temperature for three days. Following this, the silicone-epoxy topcoat (Lotus Dry) was spray-applied onto the cured gelcoat surface. The average dry thickness of the gelcoat and coating were approximately 400 ± 20 µm, measured using DeFelsko's PosiTector 200 and Elektrophysik MiniTest70 coating thickness gauges.

3.5.3 Surface Characterization

Water Contact Angle (WCA) and contact angle hysteresis (CAH) were measured to evaluate surface wettability. A Kruss™ DSA100 goniometer at 25 ± 0.5 °C was used with the sessile drop technique. In this method, a 4 µL water droplet was dropped on the surface, and WCA was calculated using the Young–Laplace model. The sliding angle (SA) of water droplets was evaluated using a Krüss instrument equipped with a tilting platform. Each sample was securely mounted on the stage, and a 35 µL water droplet, selected to minimize gravitational effects [41], was deposited on its surface before the stage was gradually inclined at a rate of 60° per minute up to a maximum of 60°, until the droplet initiated sliding or rolling. The sliding angle was recorded as the stage inclination measured 0.5 seconds before the droplet began to move. Additionally, CAH was calculated by inclining and subtracting the receding contact angle from the advancing contact angle. These measurements helped to evaluate how the surface interacted with water, reflecting its hydrophobic properties.

3.6 Evaluation of the Mechanical Durability of the Coating

A variety of tests were conducted to assess the mechanical durability of the coating, including tensile testing, rain erosion, and abrasion resistance. These assessments aimed to evaluate the coating's mechanical durability, wear resistance, and stability under simulated environmental conditions.

3.6.1 Tensile Strength

A tensile test is a key method for evaluating the mechanical properties of the coating, specifically its tensile strength, elongation, and flexibility. In this test, according to ISO/TS 19392-1, five free films of the coating were subjected to a controlled, uniaxial force until failure, providing essential data on the material's ability to resist deformation and fracture under stress at room temperature. Additionally, five samples were tested at low temperature (-35°C) to assess the coating's performance under varying thermal conditions.

3.6.2 Rain Erosion

Wind turbines are constantly subjected to high-velocity rain, which can cause significant wear on their surfaces, potentially leading to performance degradation and increased maintenance costs. Thus, the rain erosion test is a crucial evaluation method to assess the durability of coatings, especially for applications exposed to harsh environmental conditions. Referring to ISO/TS 19392-3, rain erosion is assessed by subjecting the surface to high-speed water jets or impacting droplets, reflecting the conditions of droplets hitting wind turbine blade tips at speeds up to ~90 m/s [42] (Figure 3.2). This test was carried out for three coated beams for 6000 impacts at 160 m/s, which is higher than the 90 m/s droplet velocity. The higher velocity is used to accelerate damage and ensure reproducible evaluation.

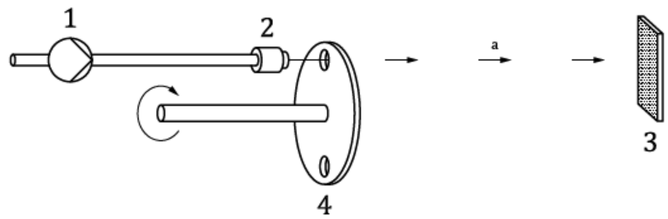

Figure 3.2. Schematic of the principle of rain erosion test device (provided by ISO/TS 19392-3:2018); 1: high-pressure pump, 2: jet nozzle, 3: panel holder, 4: rotating disc, a: fluid jet [15].

3.6.3 Abrasion Resistance

The abrasion resistance of a coating is critical for evaluating its durability against mechanical wear. The abrasion resistance test, performed as per ASTM D4060, involved 1000 cycles of a CS-17 abrasive rotating wheel under a 1 kg load at 60 rpm to simulate mechanical wear on the coating. The measurement of weight loss after 1000 abrasion cycles provides valuable insights into the material's resistance to abrasion, indicating how well the coating can withstand wear under mechanical stress.

3.7 Assessment of Coating Icephobicity

To comprehensively evaluate the icephobic performance at the laboratory scale, five complementary tests were carried out on the coated surfaces. This includes measuring ice adhesion strength using centrifugal force, performing a push-off test, subjecting the samples to repeated icing/de-icing cycles to assess durability, and determining both the ice nucleation temperature and freezing delay time. This multi-test strategy was not only intended to enhance the accuracy of the study but also to establish correlations among the results, thereby providing deeper insights into the coatings' icephobic behavior.

3.7.1 Ice Nucleation Temperature

Samples were prepared by applying a thin, uniform layer of the test coating (gelcoat or Lotus Dry) to Tzero aluminum pans, which was then allowed to dry thoroughly. Once the coating was set, a 5 mg droplet of deionized water was carefully placed at the center of each coated pan.

The samples were then subjected to a controlled cooling cycle using a TA Instruments DSC 250. The temperature decreased from 40 °C to −40 °C at a constant rate of 5 °C/min. During the cooling process, the ice nucleation temperature (INtemp), the point at which the water droplet froze, was identified by an exothermic peak in the DSC thermogram. This temperature, recorded with a precision of ±0.05 °C, was used to evaluate the nucleation behavior of each surface coating.

3.7.2 Freezing Delay Time

The freezing delay time was determined by measuring how long a 5 µL water droplet remained unfrozen on coated aluminum coupons. Experiments were conducted at –15 °C using a Krüss™ DSA100 goniometer equipped with a Peltier plate, within a controlled cold chamber. To minimize condensation effects, humidity in the chamber was regulated using anhydrous calcium sulfate desiccants. The final freezing delay time represents the average of five measurements taken from different locations across multiple samples.

3.7.3 Push-off

A custom-made device was used to measure the τice of Gelcoat and Lotus Dry coatings at −10.0 ± 0.2 °C. Figure 3.3 shows the setup of the push-off test. Deionized water was poured into a solid plastic cylindrical mold (22 mm in diameter), which was placed on top of aluminum plates coated with the test material (size: 10 × 10 cm^2). The mold stayed in place during freezing and testing to keep the ice in shape and contact area consistently. To make sure the ice fully froze into a solid cylinder, the samples were kept in a cold chamber overnight at −10.0 ± 0.2 °C.

During the test, a fixed probe was used to push the ice cylinder from the side. The probe and load cell (which measures force) stayed still, while the substrate with the ice was slowly pushed horizontally using a worm screw powered by a stepper motor. The speed of movement was 0.5 mm per minute to obtain a quasi-static load. The load cell recorded the pushing force over time.

Before the test began, the height of the probe was carefully adjusted so it touched the side of the ice just above the coated surface. The highest force recorded (F) before the ice detached was used to calculate the shear adhesion strength using Equation (1).

Equation (1): τ ice = F / A

where A is the area of contact between the ice and the coating. This method makes it easy to repeat the test and get reliable results on how well the coating resists ice sticking.

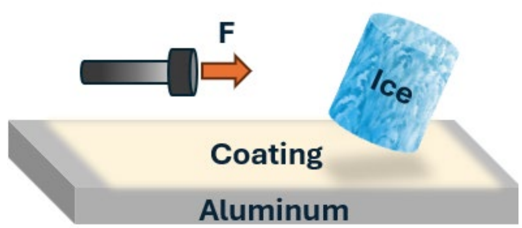

Figure 3.3. A schematic of Horizontal push-off test mechanism.

3.7.4 Icing/De-icing Cycles

The durability of the coated surfaces was evaluated by repeating the push-off test 50 times, with τice measured every 5 cycles to monitor performance over time. To ensure consistency, a custom-made plastic mold was used to form ice in a previously determined fixed area on each sample. The mold had a cylindrical cavity with a 22 mm diameter and was positioned using an alignment frame or guide, allowing it to be placed in the same location during each cycle. This setup confined the water to the same spot and ensured that the ice column had a uniform shape and contact area throughout all tests, allowing for accurate and repeatable measurements of ice adhesion.

3.7.5 Centrifugal Adhesion Test (CAT)

Centrifugal force testing was performed to determine the shear stress required to detach ice samples at a slightly large scale and for more representative atmospheric icing conditions. CAT tests were conducted using aluminum beams (6061-T6 alloy, 340×31.8×6.4 mm) rotated by an electrical motor.

Two sets of specimens were prepared: one set consisting of aluminum substrates coated with the polyester gelcoat (VIBRIN G290AA), and a second set coated with the Lotus Dry icephobic coating. Each group included three replicate samples.

To simulate natural icing, all samples were exposed to freezing drizzle (320 µm mean volumetric diameter) at an icing intensity of 11 g/h for 35 minutes and tested for two temperature conditions: –5 °C and –12 °C, representing glaze and mixed ice formation, respectively [43,44,45]. During each CAT test, beams were mounted individually in a centrifuge vat and spun from zero up to the ice detachment point at a constant acceleration of 300 rpm/s. To assess centrifugal ice-shedding, the acting force was determined using Equation (2), taking into account the ice's mass (m), radial position of the center of mass (r), and angular velocity at detachment (ω):

Equation (2): $F=mr\omega 2$

The corresponding centrifugal τice was determined by normalizing this force over the surface area in contact with the ice.

3.7.6 Spinning Rotor Blade (SRB)

The SRB is a vertical-axis spinning model consisting of a 2000 RPM, 10 hp motor, a 1-inch diameter power steel shaft, a hub, and two blades, with an overall diameter of 0.780 m. The rotating blades are mounted in the Anti-icing Material International Laboratory (AMIL)'s icing wind tunnel, a low-speed facility capable of reproducing cloud conditions with supercooled water droplets. Beyond conventional icing tests, the SRB setup can also be employed for hybrid test configurations, as discussed by Villeneuve et al. [36]. The detailed specifications of the rig are described by Fortin et al. [46]. The spinning rotor blade test [46] allows to study of passive ice protection systems under simulated conditions closer to those encountered in application. The test involves keeping the rotor at a constant rotation speed while exposing it to in-cloud icing conditions. Key ice accretion physics on rotors are captured in the test such as high droplet impact velocity, presence of centrifugal and aerodynamic forces, and efficient dissipation of thermal energy. The test is continued until ice shedding occurs at which point measurements are taken to evaluate τice from Equation (3):

$$\text{Equation (3): } \tau_{au\_ice} = \frac{\left(\left[m*\left(r-\frac{lc}{2}\right)*\omega^2\right]-[\sigma*e*s]\right)}{lc*S}$$

Where, m: Mass of shed ice, r: Rotor radius (0.391 m), σ: Cohesive normal stress of the ice (500 000 Pa), s: Curve length (0.01 m), lc: Ice shedding length (m) (measured after shedding), ω: Rotation speed during icing and shedding (rad/s) (controlled), e: Ice thickness at shedding position (m) (measured after shedding). In the scale-up process of ice adhesion testing, the SRB test marks a turning point where ice failure is no longer fully adhesive. Although the ideal failure scenario for the test is one where the full iced surface area shears off at the lowest ice thickness, in most cases, only a fraction of the ice-covered surface detaches from the blade. The failure mode is mixed where at a specific point, ice will fracture both cohesively through the thickness and adhesively along the interface towards the blade tip.

The coated blade's performance was evaluated against that of uncoated Aluminum blades under controlled experimental conditions at a constant rotational speed of 2000 RPM to obtain similar tip speed than a real V90 wind turbine blade, across two icing scenarios with ambient temperatures of –5°C and –10°C, as outlined in Table 3.1.

Table 3.1. Test Conditions for Coating Evaluation at Two Temperatures by the SRB method.

Condition	IWT				SRB			
	Speed m/s	Temperature °C	LWC g/m³	MVD µm	SRB Speed RPM	Blade Tip Speed m/s	Blade Tip speed km/h	AOA °
1	10	-5	0.5	25	2000	80	300	0
2	10	-10	0.5	25	2000	80	300	0

3.7.7 Large Scale Rotating Ice Accretion and Shedding Test Bench

Comprehensive lab-scale characterization is essential for establishing a performance baseline for ice protection coatings under controlled and repeatable conditions. While these tests offer high precision and environmental control, they may lack representativity of full-scale operational environments. Bridging this gap is key to evaluating coating performance for wind turbine ice protection and understanding the extent at which it can be efficient to identify future improvement needs. In this study, a large-scale test bench is therefore used to characterize ice shedding with the presence of the coatings in a more representative way and establish a scale-factor correlation of the coating properties to help predict its effect at full scale.

The large-scale test bench is a centrifugal adhesion test bench composed of a horizontal axis 2.6m diameter rotor equipped with two NACA 0012 blades. Testing is performed in two separate phases. First, the ice is accumulated on the rotor under controlled freezing rain precipitation at a slow rotation speed. Second, precipitation is stopped, and the iced rotor is slowly accelerated at 10 rpm/s until the ice detaches from the blades by centrifugal force. Similar to the procedure described for the SRB in Section 2.5.6, τice is determined by subtracting the cohesive portion of the failure from the total centrifugal force acting on the detached ice block. This is achieved by precisely measuring the cohesive fracture surface with a three-dimensional numerical scanner and combining it with the estimated ice cohesion strength to calculate the cohesive force. The adhesive surface area is also obtained using during the scanning process. The estimated cohesive strength of the ice is obtained using a secondary tensile test apparatus [47] under the same experimental conditions. During the icing phase, rotating cylinders are positioned near the rotor to accrete ice simultaneously and a tensile test is used to obtain the corresponding cohesive strength of the ice. The rotor blades can be changed to evaluate different substrates and characterize the performance of different ice protection systems at a larger scale. The rotor stand is installed in a tall cold chamber that includes vibration sensors, temperature probes at four different heights in the chamber, surveillance cameras, high-speed camera and a spraying ramp at the upper most point of the chamber, as depicted in Figure 2.4 This system is equipped with numerous protective equipment and enclosed in a protective cage. A spraying system is installed at eleven meters from the ground in the cold room to simulate ground atmospheric icing. The system consists of 6 Spraying Systems sprinklers disposed in line to cover the entire width of the rotor from above which can be set to simulate a wide range of icing intensity and droplet MVD. After ice shedding, blades are weighed once more to measure the mass of ice shed and the cohesive and adhesive surface areas of the failure are obtained by 3D scanning. Ice adhesion is then estimated using the same equation presented earlier for the SRB (Equation 3). Figure 2.5 shows an example of ice accumulation on the blades and numerical model of the ice resulting from the three-dimensional scan operation used to measure the ice shape and analyze its type. It also includes the corresponding post-shedding numerical scan, where the highlighted regions clearly indicate the adhesive fracture area, one of the primary areas of interest, along with the much smaller cohesive zone observed at the fracture point.

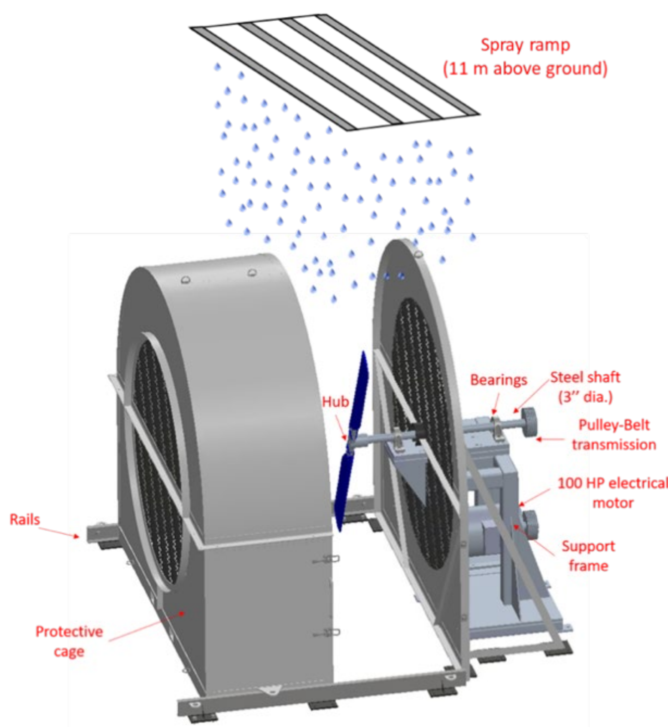

Figure 3.4. Diagram of the large-scale test bench inside the cooling chamber.

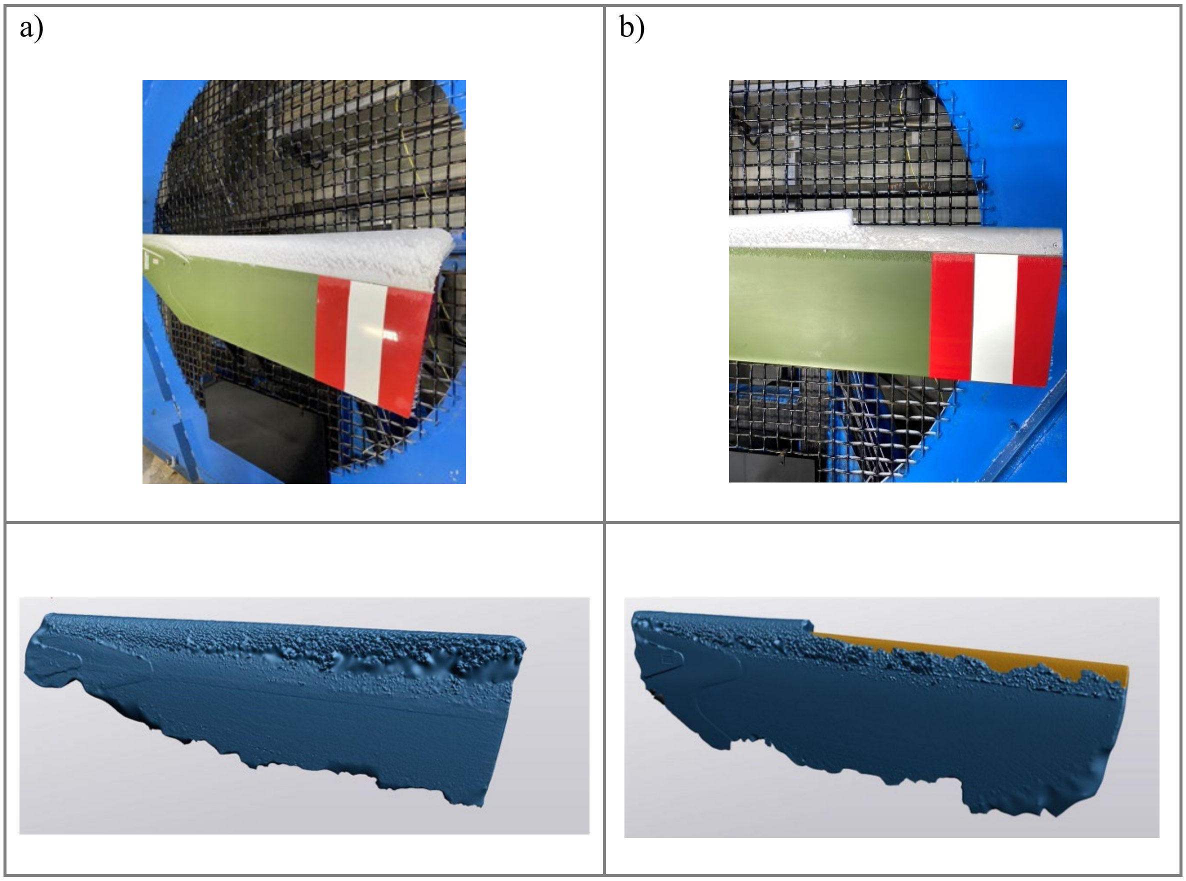

Figure 3.5. a) Iced rotor blades after accumulation phase and corresponding numerical model. b) Iced rotor blades after shedding phase and corresponding numerical model with highlighted adhesive fracture area.

3.8 Results and Discussion

3.8.1 Surface Characterization

The water contact angle, CAH and sliding angle results are presented in Table 3.2. The Lotus Dry coating exhibited a contact angle of approximately 100° and a CAH of 10°, classifying it as hydrophobic [83]. In comparison, the reference Gelcoat showed a lower WCA and higher CAH. Although low CAH is an important indicator of ice-repellent behavior and places the Lotus Dry coating within the category of icephobic surfaces [18,49], it alone does not confirm icephobicity. Therefore, further tests are conducted to validate its icephobic performance. This dual classification demonstrates the coating's potential for applications requiring both high hydrophobicity and efficient water shedding.

Table 3.2. Surface Characterization

Item Description	Lotus Dry	Gelcoat
WCA	~100° ± 2.2	~ 84° ± 1.9
CAH	~10° ± 1.6	~55° ± 1.2
Sliding angle	~18° ± 0.3	~30° ± 0.4

.

3.8.2 Evaluation of the Mechanical Durability of the Coating

3.8.2.1 Tensile Strength

According to the test results presented in Figure 3.6, the coating free films behave as a brittle material, fracturing with little to no elastic deformation at both room and –35 °C. The elongation at break was consistently low, averaging 1.25% at room temperature and 0.53% at low temperature, both below 2%, which reflects their limited flexibility. Additionally, the Lotus Dry coating showed low yield strength, averaging 10.9 MPa at room temperature and 8.9 MPa at low temperature. Notably, the Gelcoat could not be characterized by tensile testing due to its extremely fragile nature.

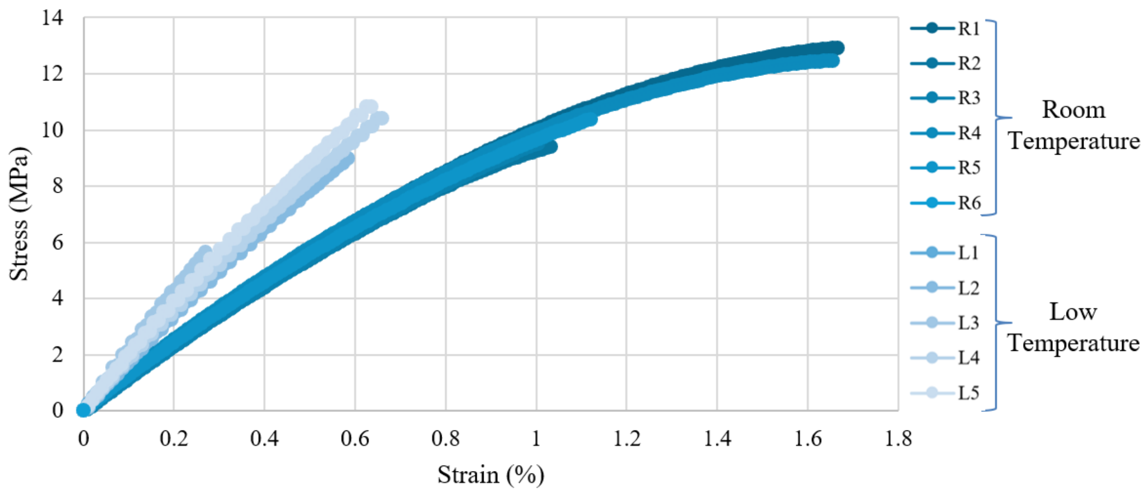

Figure 3.6. Tensile Test Results at both room and -40°C temperatures.

These findings suggest that, while the coating performs better than the Gelcoat, it still lacks sufficient elasticity, an essential property for applications involving rotating components such as wind turbine blades. In such systems, coatings must withstand dynamic forces from rotation, vibrations, particle impacts, and environmental stresses. High elongation at break is therefore a key requirement to ensure long-term durability and mechanical reliability. To address this limitation, future modifications should focus on improving the coating's mechanical strength, with particular attention to enhancing its elongation properties. While improving elongation at break is essential for withstanding mechanical stress from rotation and impacts, it is also important to consider wear resistance. Excessively soft and elastic coatings may degrade faster under environmental exposure and mechanical erosion. A balanced mechanical profile, combining sufficient flexibility to prevent cracking with adequate hardness to resist wear, would be ideal. Therefore, future work should aim to optimize both elongation (>10%), as suggested in previous studies [18], while maintaining adequate hardness to ensure long-term durability.

3.8.2.2 Rain Erosion

The performance of the developed coating under rain erosion conditions is summarized in Table 3.3. According to the standardized evaluation method outlined in ISO-TS-19392-2:2018, the coating qualifies as durable surface, owing to its consistent performance throughout the testing process.

The coating endured over 6000 water droplet impacts at a jet velocity of 160 m/s, simulating the harsh weathering conditions typically faced by wind turbine blades. Notably, no visible surface degradation, delamination, or loss of functionality was observed, demonstrating excellent mechanical resilience and surface stability under high-velocity impact.

Although tensile testing revealed that the coating behaves as a brittle material, showing low elongation at break and no plastic deformation, its strong performance under rain erosion suggests a more complex mechanical response. The ability to resist localized, short duration impacts despite limited bulk flexibility indicates that the coating possesses sufficient surface toughness and cohesive strength to absorb and dissipate dynamic stresses. This contrast highlights that brittleness under uniaxial loading does not necessarily correlate with poor behavior under repeated impact, reinforcing the importance of evaluating coatings under multiple mechanical stress modes relevant to their application.

In contrast, the gel-coated reference samples began showing damage before 6000 impacts, including surface wear, micro-cracking, and partial coating removal. This direct comparison highlights the superior erosion resistance of the silicone-epoxy coating, which retained both its structural integrity and functional surface properties after prolonged exposure to aggressive conditions.

These findings suggest that the developed coating is a promising candidate for long-term application in high-impact environments, such as the leading edges of wind turbine blades. Its ability to withstand repeated mechanical stress without loss of performance enhances its viability as a durable passive icephobic solution, supporting improved operational reliability and reduced maintenance in cold climate energy systems.

Table 3.3. Rain Erosion Test results for both gel-coated and Lotus dry coated samples.

Samples	Number of impacts	Results
Gel Coat	< 6 000	The coating seems to come off the surface in chunks rather than at the precise points of impact
Coating	> 6 000	No evidence of surface damage

The pictures of coated beams after the rain erosion test are presented in Figure 3.7:

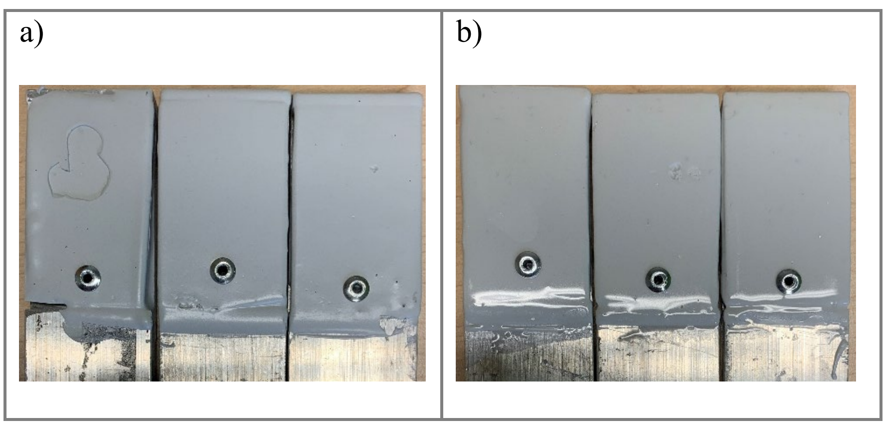

Figure 3.7. Rain erosion test results showing the performance of a) the eroded gel-coated surfaces and b) the epoxy-silicone coated sample, which remained non-eroded.

3.8.2.3 Abrasion Resistance

All three samples demonstrated excellent abrasion resistance, with an average wear index of 72 mg/1000 cycles and no significant material loss or visible surface degradation after testing (Figure 3.8). These results should be interpreted in the context of the unique characteristics of silicone-epoxy systems. Unlike neat, rigid epoxy formulations, silicone–epoxy hybrid coatings are distinguished by their low surface energy and inherent flexibility. Neat epoxy coatings typically exhibit a substantially higher wear index of approximately 115 mg/1000 cycles, indicating a more brittle failure mechanism and greater mass loss [50,52] . The relatively lower wear index of the silicone-epoxy coatings, combined with the absence of delamination or visual degradation, suggests that wear occurs primarily through controlled surface deformation rather than fracture or particle loss. These findings highlight the distinctive wear behavior of silicone-epoxy coatings and their suitability for applications such as wind turbine blades, where coatings are expected to undergo prolonged mechanical stress and environmental exposure while preserving key functional properties.

Figure 3.8. Surface of the coating after abrasion test, exhibiting minimal wear and no significant damage.

3.8.3 Assessment of Coating Icephobicity

3.8.3.1 Ice Nucleation Temperature

Figure 3.9 shows that the developed coating had a lower average ice nucleation temperature (-16.7±0.05 °C) than the reference gelcoat (-14.5±0.03 °C), based on measurements from three independent samples of each, suggesting delayed ice formation. This behavior can be attributed to its low surface energy, hydrophobicity, and flexible silicone-rich domains, which reduce the likelihood of water molecules organizing into a stable ice nucleus at the interface compared to the more rigid and polar polyester Gelcoat surface. As a result, the coating not only delays ice nucleation but also plays a significant role in minimizing ice accumulation and facilitating ice removal after formation.

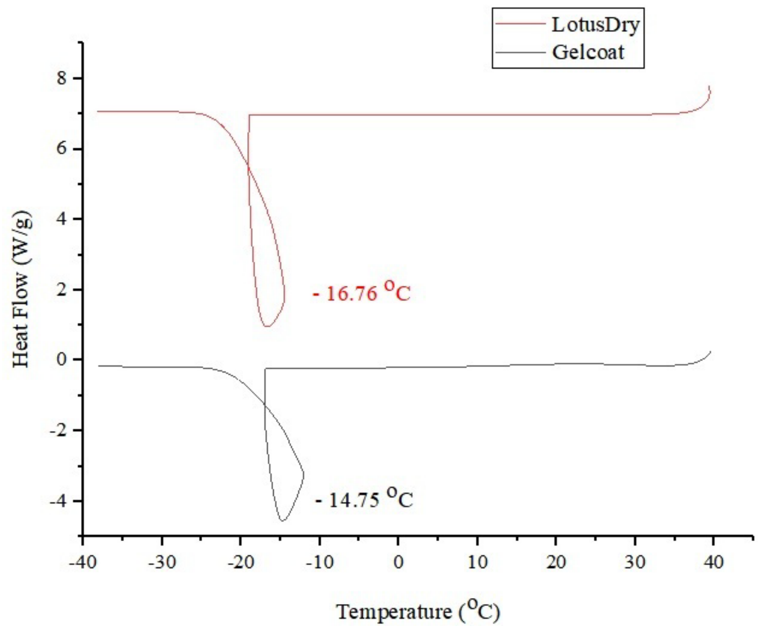

Figure 3.9. The average ice nucleation temperatures (INtemp) for the Gelcoat and Lotus Dry coatings.

3.8.3.2 Freezing Delay Time

The silicone-epoxy coating delayed ice formation by approximately 1,020 seconds in a controlled environment at -15 °C, compared to 540 seconds for the Gelcoat. This prolonged freezing time is a clear indication of the coating's superior resistance to ice nucleation, which is a critical factor in the development of effective anti-icing surfaces. By impeding the initial formation of ice crystals under subzero conditions, the coating significantly enhances operational reliability and safety, especially in scenarios where ice accumulation can lead to mechanical failure or reduced system performance. The ability to delay freezing not only minimizes the frequency of required maintenance interventions but also contributes to energy savings by reducing the need for active de-icing methods such as heating or chemical treatments. Beyond this improvement, the coating also demonstrates promising anti-icing behavior, as evidenced by its low τice and efficient ice-shedding capability, which are detailed in the following sections. Figure 3.10 illustrates the frozen water droplet on the silicone-epoxy coated coupon after 1020 seconds at -15 °C.

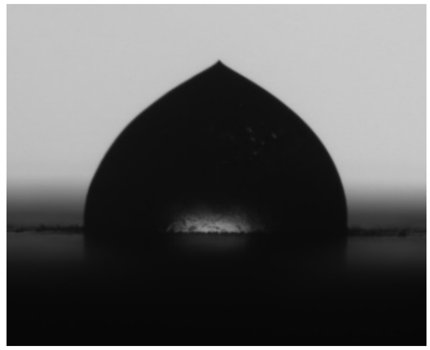

Figure 3.10. Frozen water droplet on the surface of the coated coupon after 1020 seconds at -15°C.

3.8.4 Push-off Adhesion Test

Three coated samples were prepared, and τice of an ice mold on each surface was measured using a custom-built push-off test. The Lotus Dry-coated substrates exhibited an average τice of 8.3 ± 1.1 kPa, remaining well below the 20 kPa benchmark [53,55]. In contrast, the gelcoat showed a significantly higher τice of 13.7 ± 3.9 kPa, although still below 20 kPa benchmark. For reference, bare aluminum displayed a much higher τice of 128.9 ± 11.9 kPa. These findings suggest that lateral shear detachment is strongly influenced by surface chemistry. The substantial reduction in push-off force for Lotus Dry-coated samples indicates excellent practical ice-shedding potential, as surfaces with τice values below 20 kPa are typically considered optimal for anti-icing applications [37,56].

Throughout 50 icing/de-icing cycles which carried out by a home-made push-off device, the average τice remained consistently low, 19.6 ± 3.6 kPa for the Lotus Dry coating, as illustrated in Figure 3.11. The consistently low values of τice (below 20 kPa) observed throughout these tests indicate that the coating's icephobic properties were well-preserved, ensuring reliable performance over extended periods of exposure to icing conditions [57,62]. Notably, the long-term stability and durability of its anti-icing functionality make it well-suited for use on wind turbine blades and other critical outdoor infrastructure exposed to severe winter weather. This reliability can contribute to enhanced operational performance, reduced downtime, and lower maintenance costs, underlining the coating's strong potential for large-scale deployment in cold-climate technologies.

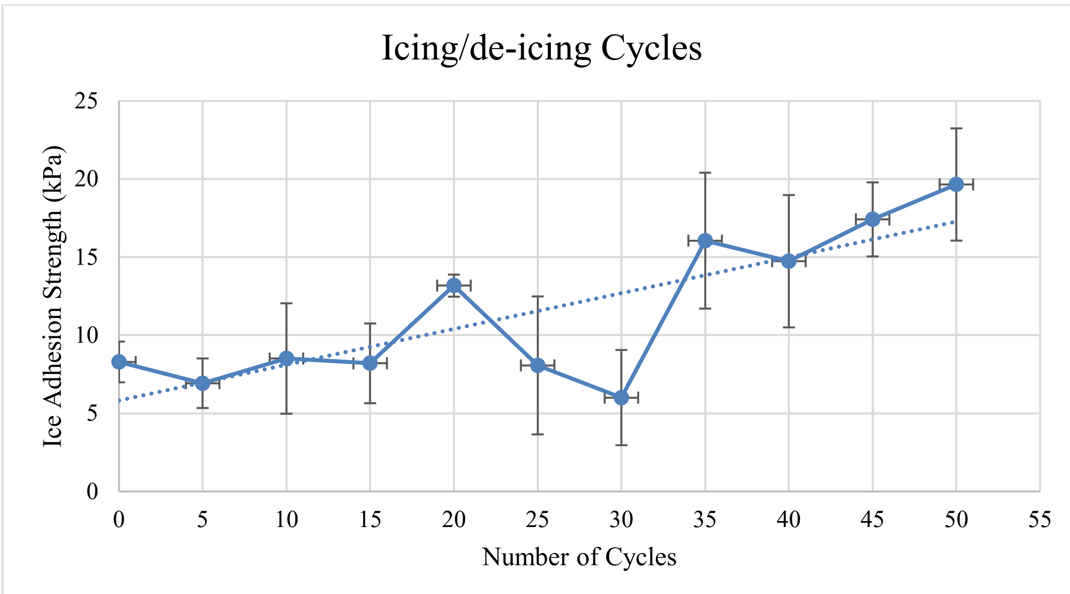

Figure 3.11. Ice adhesion strength of the silicone-epoxy coating after 50 icing/de-icing cycles.

3.8.5 Ice Adhesion Performance Across Conditions and Test Methods

The different ice adhesion assessment methods presented were tested under two conditions, warmer (−5 °C) and colder (−10 to −12 °C) temperatures. Due to the differences in scale, ice types and ice detachment modes, the comparison of these methods is rendered a complex but hugely insightful analysis. The following section presents the shapes and types of ice obtained at different temperatures for each ice adhesion test as well as the type of detachment for each sample. The test samples appearance is greatly influenced by the precipitation parameters, rotation speed, and the type of fracture that leads to the ice shedding.

Figures 3.12 and 3.13 present result examples for the CAT tests at -12°C and -5°C respectively. Results at warmer temperatures involve mostly purely adhesive failure, while the second type of failure (cohesive), typically obtained at colder temperatures (Figure 3.13). The cohesive failure for aluminum substrates as can be observed in Figure 2.12b, while gelcoat and Lotus Dry retained adhesive predominant failure modes (
Figure 3.12c and d).

Figures 3.14 and 3.15 show ice formation under both conditions and the types of ice shedding for the SRB and large-scale test benches. As shown in Figure 3.13a the substrate wettability significantly affected the ice formation process under warmer accumulation conditions, due to the presence of a wet regime, resulting in non-uniform ice growth. This can significantly influence the measured adhesion strength during testing. This was not observed for the large-scale rotor and SRB, probably this is explained by the air flow caused by the rotation, improving dissipation of latent heat and impact ice formation vs ground icing (CAT).

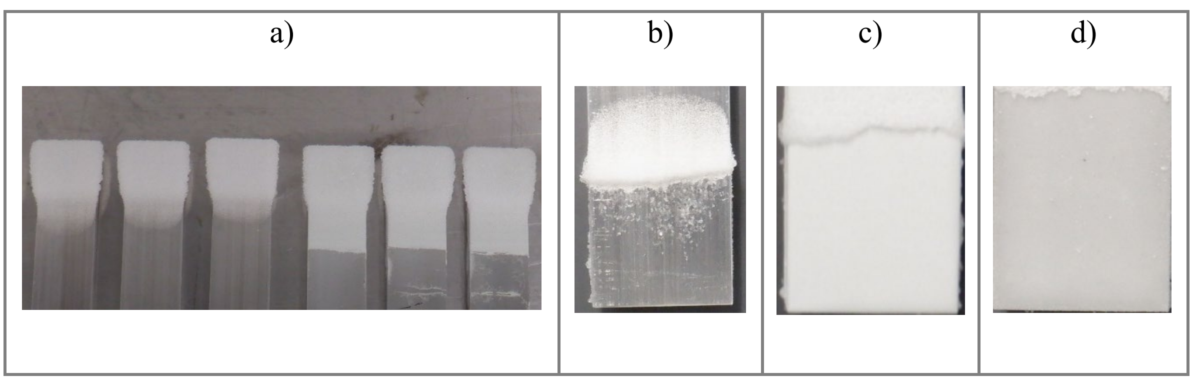

Figure 3.12. a) CAT blades ice accumulation in -12ºC on aluminum, gelcoat and Lotus Dry. b) Example of CAT blade result at -12ºC on aluminum showing partial ice detachment c) Example of CAT blade result at -12ºC on gelcoat with minor ice residual. c) CAT blade result in -12ºC on Lotus Dry showing adhesive failure with complete ice detachment.

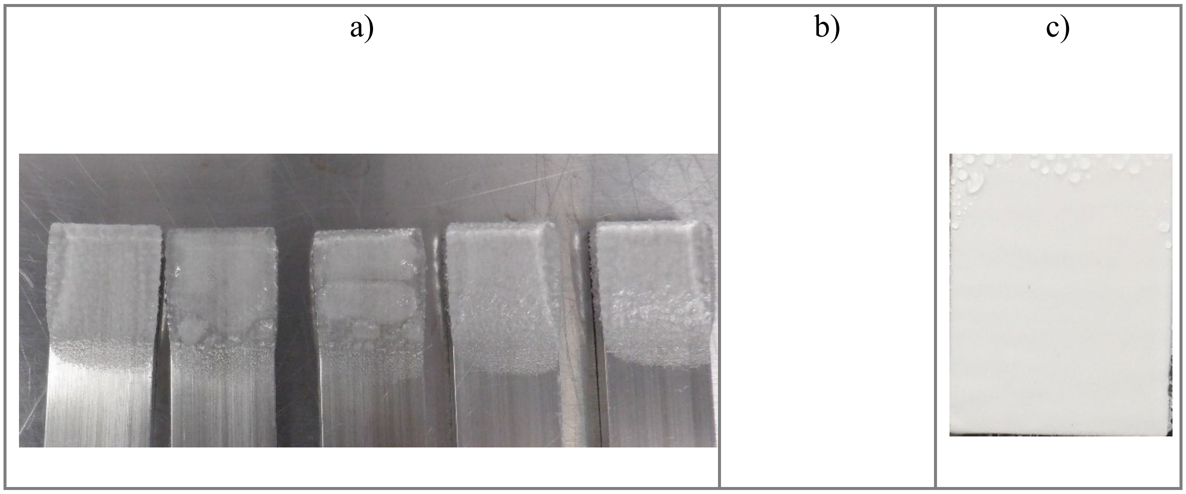

Figure 3.13. a) CAT blades ice accumulation in -5ºC on aluminum with inconsistent solidification. b) CAT blade result in -5ºC on aluminum. C) CAT blade result in -5ºC on Lotus Dry with complete ice detachment.

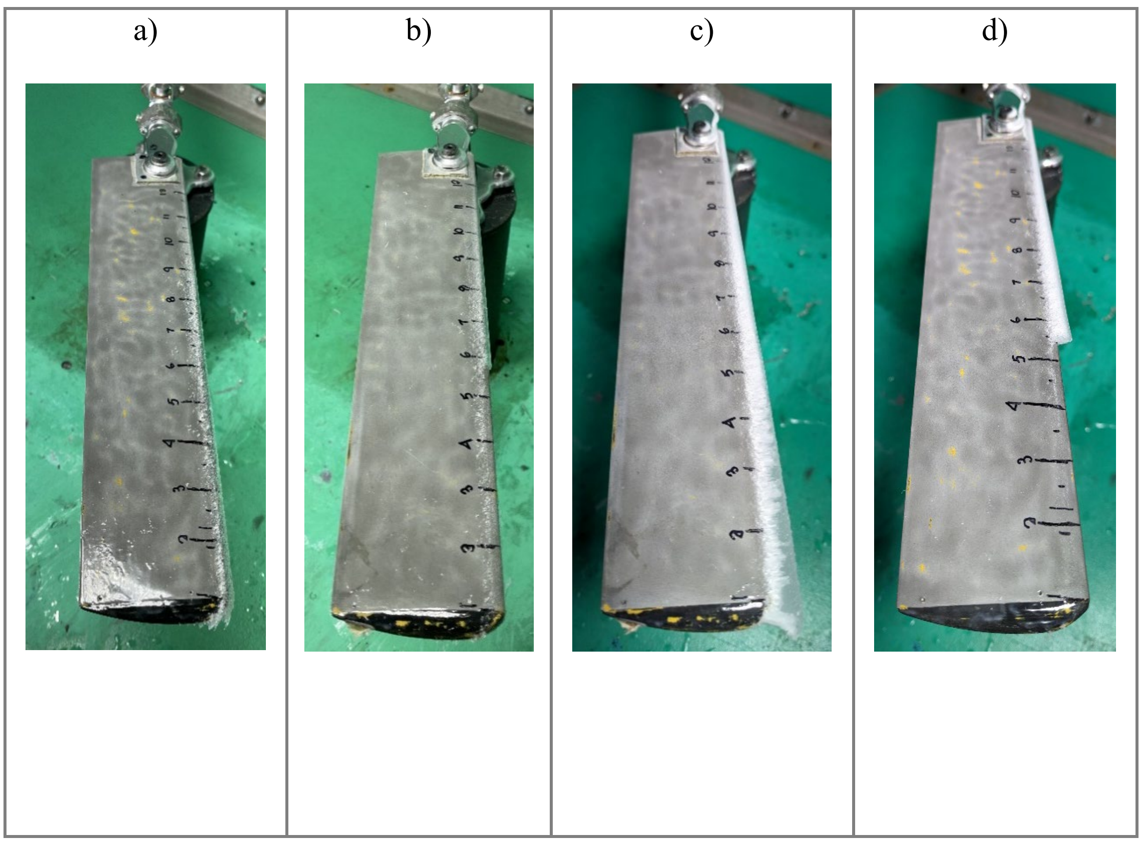

Figure 3.14. a) Ice accumulation on SRB blade at -5ºC for Lotus Dry. b) SRB test result at -5ºC for Lotus Dry, c) Ice accumulation on SRB blades at -12ºC on Lotus Dry, d) SRB test result at -12ºC on Lotus Dry.

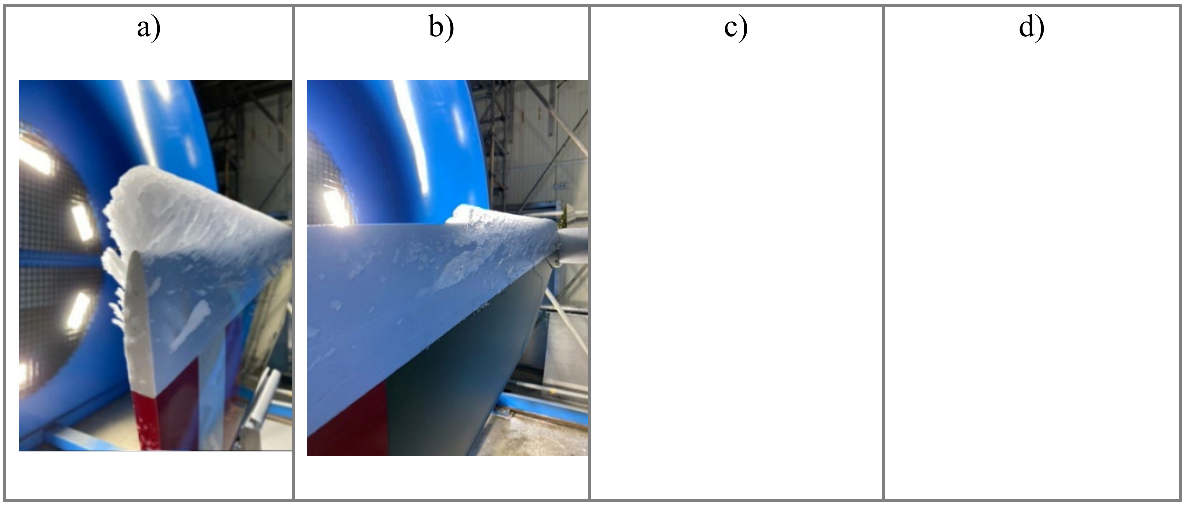

Figure 3.15. a) Ice accumulation on Large-scale blade in -12ºC on Lotus Dry. b) Large-scale test result in -12ºC on Lotus Dry. c)Ice accumulation on Large-scale blade in -5ºC on Lotus Dry. d) Large-scale test result in -5ºC on Lotus Dry.

Push-off adhesion failure results were excluded from this comparison since the ice used was molded rather than atmospheric, and the applied strain rate did not represent the failure conditions of the other tests. Also, since the ice studied here was produced while simulating atmospheric accretion, with droplets freezing upon contact, factors such as freezing delay and nucleation temperature are not relevant for this analysis and are also not considered.

A detailed analysis of the ice adhesion data under both conditions reveals distinct performance trends across different substrate types and testing methods, as summarized in Table 3.4. The following discussions explore the influence of substrate composition, temperature variation, and consistency across testing methods, supported by quantitative comparisons to highlight the reliability and significance of the results.

Table 3.4. Ice adhesion strength of various substrates measured at different temperatures (-5 °C to -12 °C) using multiple testing methods.

Samples	Tests	τ ice at warmer Temperature (-5°C)			τ ice at colder Temperature		
		CAT MPa	SRB MPa	Large-scale MPa	CAT (-12°C) MPa	SRB (-10°C) MPa	Large-scale (-12°C) MPa
Aluminum		0.29±0.04	0.11±0.002	0.17±0.06	0.54±0.081	0.230±0.03	0.25±0.04
Gelcoat		0.27±0.05	-	0.11 ±0.01	0.47±0.07	-	0.16±0.02
Lotus Dry		0.076±0.05	0.027±0.009	0.05±0.03	0.146±0.01	0.101±0.049	0.06±0.03

CAT tests at -12°C for aluminum were corrected by removing the cohesive component from the centrifugal force at failure, like the method described for SRB.

3.8.5.1 Inter-method Correlation and Reliability

A comparative analysis of CAT, SRB, and large-scale results reveals key insights into the reliability and representativity of each method. For the aluminum results, SRB and large-scale test values showed significant alignment. When compared to CAT, the SRB and large-scale tests resulted in lower adhesion values, averaging about 58% lower (SRB) and 57% lower (large-scale) than CAT results. For instance, at -12°C, CAT measured 0.54 MPa on aluminum, compared with 0.25 MPa for large-scale (a difference of 116%), while for Gelcoat the gap was even larger (0.47 vs 0.16 MPa, 194% higher). In contrast, SRB and large-scale results were much closer to each other, differing on average by less than 10%, which suggests that these two methods yield consistent results as the test is scaled up.

CAT differs in that failures involve the complete detachment of the ice, whereas SRB and large-scale tests typically produce a combination of cohesive and adhesive fracture as only a portion of the ice sheds. It is worth noting that these differences are influenced not only by the scale of the setups but also by the geometry of the test specimens. In both the large-scale and SRB tests, ice forms around the curved leading edge of the blade and tends to detach through a mix of adhesive and cohesive failure. In contrast, the CAT test forms ice on a flat surface with a shorter interface, with the adhesion plane parallel to the direction of spinning, leading more often to purely adhesive failure. In SRB and large-scale methods, it is assumed that at failure, the centrifugal load is equal to the combined adhesive and cohesive limits of the ice acting over the area of the shed piece. However, this assumption neglects fracture mechanics and material defects, where failure may initiate and propagate either within the ice volume or along the interface. This could explain why adhesion strength values from SRB and large-scale tend to be underestimated relative to CAT. Further investigation into the fracture mechanics of partial ice detachments is needed to establish a more accurate relationship between the adhesion strength measured by CAT and the partial shedding observed on more complex structures.

Interestingly, the trends across the three measurement methods are consistent. Using the adhesion reduction factor (ARF), defined here as how many times adhesion on aluminum is higher than on Lotus Dry, Lotus Dry is shown to significantly reduce adhesion. At warmer temperatures, ARF values range from 3.4 to 4.1, indicating that adhesion on aluminum is over three times greater than on Lotus Dry. At colder temperatures, CAT and large-scale tests show ARFs of 3.7 and 4.2, respectively. These consistent reductions suggest that while CAT may better capture adhesion strength as an intrinsic material property, the adhesion reduction is also clearly reflected in the more realistic SRB and large-scale methods.

Large-scale and SRB test benches both have partial shedding of the ice when the rupture point is attained. Because of their difference in size, this behavior can be used to analyse the shedding ratio and extrapolate to build predictions on the behavior of the ice on full scale wind turbines. Table 3.5 presents a comparison of the ice shed length for both testing methods.

Table 3.5. Ice Shedding Length in Partial Failure Mode Comparison for Large-Scale Tests and SRB Tests on All Substrates.

Temperature (ºC)	Substrate	Average Shed Length (mm)		Percentage of blade length shed (%)		Standard Deviation (%)	
		Large-scale	SRB	Large-scale	SRB	Large-scale	SRB
-12	Aluminum	362	89	28%	28%	2%	5%
	Gelcoat	352	N/A	27%	N/A	7%	N/A
	Lotus Dry	366	100	28%	32%	17%	7%
-5	Aluminum	334	146	26%	46%	4%	5%
	Gelcoat	388	N/A	30%	N/A	5%	N/A
	Lotus Dry	305	126	23%	40%	10%	1%

Large-scale and SRB testing differ in their approaches but provide complementary insights. In large-scale testing, ice is accreted to a target thickness at low rotation speeds, after which the speed is gradually increased until shedding occurs. This procedure simulates a wind turbine that has accumulated ice under light wind conditions and later attempts to operate in stronger winds. For passive coatings, the desired performance is early shedding at low rotational speeds combined with high shedding coverage. By contrast, SRB testing involves ice accretion while the blade is already rotating at a constant speed, representing operation in sustained high winds. In this case, shedding occurs once a critical ice mass is reached. For passive coatings, the goal is to minimize the ice mass required to trigger shedding while maximizing the proportion of the blade that sheds.

In terms of shedding behavior, the percentage of shed length is comparable between SRB and large-scale at –12°C. However, at the warmer condition (–5°C), SRB exhibits larger shed lengths. This aligns with the reduction in ice adhesion at warmer temperatures, which facilitates more extensive shedding. The absence of a comparable increase in large-scale testing may be attributed to the delay between ice accretion and centrifugal loading, as well as the greater thermal mass of the larger blades. This delay allows the ice to stabilize at the ambient –5°C. In contrast, SRB testing is more dynamic: the thin aluminum-skinned blades are more susceptible to heating effects, and the latent heat of fusion released during ice accretion can raise the interfacial temperature. As a result, the effective interface temperature in SRB may be higher than in large-scale testing under the same ambient conditions, favoring earlier and more extensive shedding.

For the Lotus Dry coating, its reduced adhesion translates into shedding at lower loads (lower RPM in large-scale and lower accreted mass in SRB). However, shedding lengths are not significantly different from aluminum, suggesting that adhesion alone does not fully dictate the extent of shedding. Shedding typically occurs in the tip-most region of the blade, which is beneficial for the recovery of aerodynamic performance in wind turbine applications. Maximizing shed length while minimizing adhesion strength therefore represents a promising direction for future coating development. Equally important is the need to better understand the stress states that govern ice shedding. The discrepancies observed between adhesion measurements from CAT, SRB, and large-scale methods indicate that mechanical considerations, such as static versus dynamic loading, or partial-shedding (SRB, large-scale) versus complete detachment (CAT), play a key role in the adhesion strength measurements. Overall, SRB tests offer strong predictive value for field-scale adhesion behavior, particularly when assessing passive coatings under dynamic conditions. Large-scale tests are even more representative but are limited by lower test throughput and higher resource requirements. Meanwhile, CAT remains useful for material screening and assessing temperature effects but may overestimate adhesion due to its simplified loading configuration.

3.8.5.2 Influence of Substrate Composition

Across all tested substrates, aluminum consistently exhibited the highest adhesion values in CAT, SRB, and large-scale tests. For example, CAT measurements for aluminum increased from 0.290 MPa at −5°C to 0. 54 MPa at −12 °C, highlighting its strong ice-substrate bonding affinity and poor icephobic properties. Notably, CAT cold-condition results for aluminum showed cohesive failure in addition to adhesive failure (partial ice detachement), due to high ice/aluminum adhesion strength. Gelcoat showed slightly lower, yet comparable, adhesion values. On average across all testing methods, the gelcoat demonstrated an adhesion reduction factor (ARF) of 1.35 compared to aluminum.

In contrast, the Lotus Dry-coated surfaces exhibited significantly lower ice adhesion in all test configurations. CAT results showed adhesion strength of 0.076 MPa at -5 °C and 0.146 MPa at -12 °C, which are significantly lower than both aluminum and gelcoat. Notably, Lotus Dry applied on a gelcoat base layer showed the lowest adhesion under large-scale tests, with values of 0.05 MPa at -5 °C and 0.06 MPa at -12 °C. The average ARF for the Lotus Dry coating was 3.57, confirming its strong potential to significantly reduce ice adhesion on wind turbine blades.

The fact that the ARFs are stable in between test methods and show similar values for substrate comparison highlights the potential of both small scale and scaled-up testing methods and confirms that they can accurately represent substrate behavior without introducing significant error in their performance evaluations. Smaller scale tests are quick and inexpensive, great for screening multiple formulations, and larger scale setups allow to obtain a comprehensive characterisation of well-rounded products, allow to assess durability and act as a last step before field tests.

3.8.5.3 Temperature Dependence of Ice Adhesion

A general trend of increasing adhesion with decreasing temperature was observed, particularly for uncoated substrates, consistent with literature reports of enhanced adhesion at lower temperatures, typically up to a critical point around −20 °C, beyond which adhesion strength may begin to decline [63]. This trend is also influenced by changes in the ice composition: as temperatures move away from 0 °C, glaze ice exhibits stronger adhesion, but this behavior changes as conditions transition toward rime ice, which has different mechanical properties and weaker bonding [64,65]. Additionally, for all substrates tested, a greater variability in ice adhesion results was observed in warmer temperatures, especially on the Large-scale test bench. The greater variability observed at -5°C is attributed to differences in ice morphology and freezing dynamics, but also to a lesser precision for this test bench in the range of lower adhesion values.

Across all testing methods, the average increase in adhesion strength under colder conditions was 1.8 for aluminum, 1.6 for gelcoat, and 2.3 for the Lotus Dry coating. The similar trend observed for gelcoat and aluminum suggests that their adhesion increase with colder temperatures is more characteristic of the ice itself rather than the substrate. In contrast, the stronger temperature dependence observed for Lotus Dry suggests that its surface properties may accentuate thermal effects. Moreover, the Lotus Dry coating demonstrated stable adhesion performance across both tested temperatures, confirming that Lotus-based surfaces maintain consistent ice adhesion and shedding behavior. This supports their temperature-independent anti-icing effectiveness, which is a desirable feature for real-world applications in fluctuating atmospheric conditions.

In both tested conditions, the Lotus Dry is significantly less adhesive than the base substrate for wind turbines. These results support the hypothesis that ice formed at temperatures close to 0°C adheres less and demonstrate that the icephobic coating significantly reduces ice adhesion compared to the gelcoat. In the field, the application of this coating could translate into shorter downtimes for wind turbines. Lower adhesion increases the likelihood of natural ice shedding due to centrifugal forces during rotation or environmental factors such as wind and solar radiation. This passive protection system could enable turbines to resume operation more quickly after icing events or even continue spinning during moderate icing and shedding ice without requiring a complete stop. Furthermore, coatings like this could complement electrothermal de-icing systems by reducing the energy required for ice removal, particularly in areas of the blade where active systems are less efficient. This confirms its potential performance for practical application on wind turbine blades exposed to icing conditions.

3.9 Conclusion

Ice accumulation on wind turbine blades remains a critical challenge for energy efficiency and reliability. To evaluate how material properties translate into functional performance, our study assessed a commercial silicone–epoxy coating by linking mechanical strength, wettability, and freezing delay to multi-scale ice adhesion tests. Results showed that longer freezing delays and lower contact angle hysteresis correlated with improved icephobicity across push-off, CAT, SRB, and large-scale tests. Differences in adhesion values across test methods were traced to distinct adhesion-dominated versus cohesion-dominated failure behaviors. Adhesion-dominated failures, characterized by clean ice detachment from the surface, are preferable for anti-icing performance and were more frequently observed in CAT and push-off tests. On the other hand, cohesion-dominated failures, which occur within the bulk of the ice, indicate either a stronger interface or the presence of localized stress concentrations. Mixed cohesive–adhesive failures were typically observed in SRB and large-scale measurements, further reflecting the complex nature of ice detachment under realistic conditions. Overall, this study offers an integrated evaluation strategy, combining material-level properties with multi-scale testing to better predict field performance. The consistency between dynamic lab tests and large-scale outcomes validates the coating's icephobicity and underscores the need to consider both interfacial mechanics and scale when designing and evaluating anti-icing coatings. This work represents a significant step toward translating laboratory coatings into field-ready solutions for wind turbines and similar applications.

3.10 Acknowledgments

The authors gratefully acknowledge the support from the Natural Sciences and Engineering Research Council of Canada (NSERC), The authors gratefully acknowledge the support of the Natural Sciences and Engineering Research Council of Canada (NSERC), which funded this research. The authors would also like to acknowledge the Chaire Institutionnelle de Recherche en Matériaux Antigivre Innovants (CiMAGI) at the Université du Québec à Chicoutimi (UQAC) and the Laboratoire International des Matériaux Antigivre (LIMA) for providing the infrastructure necessary to carry out this work. The authors are especially grateful to Patrice Rondeau of LIMA for his assistance with large-scale testing. Finally, special thanks are extended to Techeol Co. and PRIMA-Québec for their valuable support and collaboration.

3.11 References

1. Hassan, Q., et al., *The renewable energy role in the global energy Transformations.* Renewable Energy Focus, 2024. **48**: p. 100545.
2. Lamraoui, F., et al., Atmospheric icing impact on wind turbine production. Cold Regions Science and Technology, 2014. 100: p. 36-49.
3. Rodríguez-López, M.Á., E. Cerdá, and P.d. Rio, *Modeling wind-turbine power curves: effects of environmental temperature on wind energy generation.* Energies, 2020. **13**(18): p. 4941.
4. Li, Y., et al., *Scaling method of the rotating blade of a wind turbine for a rime ice wind tunnel test.* Energies, 2019. **12**(4): p. 627.
5. Madi, E., et al., *A review of integrating ice detection and mitigation for wind turbine blades.* Renewable and Sustainable Energy Reviews, 2019. **103**: p. 269-281.
6. Wang, L., et al., *Wind turbine blade icing risk assessment considering power output predictions based on SCSO-IFCM clustering algorithm.* Renewable Energy, 2024. **223**: p. 119969.
7. Krenn, A., et al., *Available technologies for wind energy in cold climates.* International Energy Agency Wind Task, 2016. **19**.
8. Zheng, S., et al., *Durable waterborne hydrophobic bio-epoxy coating with improved anti-icing and self-cleaning performance.* ACS Sustainable Chemistry & Engineering, 2018. **7**(1): p. 641-649.
9. Nistal, A., B. Sierra-Martín, and A. Fernández-Barbero, *On the Durability of Icephobic Coatings: A Review.* Materials, 2023. **17**(1): p. 235.
10. Brassard, J.-D., et al., *Ice accretion, shedding, and melting on cable-stayed bridges: A laboratory performance assessment.* Cold Regions Science and Technology, 2022. **204**: p. 103672.
11. *ISO 527-1:2019 Plastics — Determination of tensile properties, Part 1: General principles*. 2019.
12. *ASTM D2240*. 2021.
13. *ASTM D4060-19, 2019.* . 2019.

14. *ISO/TS 19392-6:2023 Paints and varnishes — Coating systems for wind-turbine rotor blades Part 6: Determination and evaluation of ice adhesion using centrifuge*. 2023.

15. *ISO/TS 19392-3:2018 Paints and varnishes — Coating systems for wind-turbine rotor blades Part 3: Determination and evaluation of resistance to rain erosion using water jet*. 2018.

16. Geneva, I., *ISO/TS 19392-6:2023 (E); Paints and Varnishes—Coating Systems for Wind-Turbine Rotor Blades—Part 6: Determination and Evaluation of Ice Adhesion Using Centrifuge.* 2023.

17. Honarkar, H., G. Minoofar, and M. Barikani, *Effect of the type of anionic center on the characteristics of eco-friendly waterborne polyurethane/acrylate hybrids.* Monatshefte für Chemie-Chemical Monthly, 2022. **153**(12): p. 1269-1275.

18. Minoofar G, et al. Progress in icephobic coatings for wind turbine protection: Merging chemical innovation with practical implementation. Crystals 2025;15(2): 139.

19. Piscitelli, F., et al., *Superhydrophobic coatings as anti-icing systems for small aircraft.* Aerospace, 2020. **7**(1): p. 2.

20. Zhao, Z., et al., *Progress in mechanism design of functional composites for anti-ice/deicing materials.* Surface Science and Technology, 2024. **2**(1): p. 2.

21. Nemati Giv, A., et al., *Effect of reinforcements at different scales on mechanical properties of epoxy adhesives and adhesive joints: a review.* The Journal of Adhesion, 2018. **94**(13): p. 1082-1121.

22. Ziętkowska, K., et al., *Transparent Silicone–Epoxy Coatings with Enhanced Icephobic Properties for Photovoltaic Applications.* Applied Sciences, 2023. **13**(13): p. 7730.

23. Brusciotti, F., et al., *Hybrid epoxy–silane coatings for improved corrosion protection of Mg alloy.* Corrosion science, 2013. **67**: p. 82-90.

24. Shamshiri, M., R. Jafari, and G. Momen, *A novel hybrid anti-icing surface combining an aqueous self-lubricating coating and phase-change materials.* Progress in Organic Coatings, 2023. **177**: p. 107414.

25. Moghadam, S.G., et al., *In-depth analysis of the effect of physicochemical properties of ionic liquids on anti-icing behavior of silicon based-coatings.* Cold Regions Science and Technology, 2023. **216**: p. 104007.

26. Joseph, V.S., et al., *Silicone/epoxy hybrid resins with tunable mechanical and interfacial properties for additive manufacture of soft robots.* Applied Materials Today, 2021. **22**: p. 100979.
27. Adja, A.A.S., et al., *Step by step progress to achieve an icephobic silicone-epoxy hybrid coating: Tailoring matrix composition and additives.* Journal of Applied Polymer Science, 2023. **140**(32): p. e54262.
28. Shu, T., et al., *Anticorrosive and anti-icing/deicing behavior of epoxy composite coatings reinforced with GO-PPy@ SiO2 photothermal fillers.* Chemical Engineering Journal Advances, 2024. **18**: p. 100592.
29. Ziętkowska, K., et al., *Transparent Silicone–Epoxy Coatings with Enhanced Icephobic Properties for Photovoltaic Applications.* Applied Sciences, 2023. **13**(13): p. 7730.
30. Zhao, L., et al., *Icephobic Coating Based on Epoxy/Polydimethylsiloxane Interpenetrating Polymer Network Gel.* Coatings, 2024. **14**(1): p. 76.
31. Sullivan, A., X. Duan, and J. Yang, *Energy-efficient anti-icing performance of a hybrid superhydrophobic and electrothermal coating on metallic substrates.* Materials Chemistry and Physics, 2023. **301**: p. 127700.
32. Zhang, L., et al., *Robust photothermal superhydrophobic coatings with dual-size micro/nano structure enhance anti-/de-icing and chemical resistance properties.* Chemical Engineering Journal, 2022. **446**: p. 137461.
33. Cheng, T., et al., *Magnetic particle-based super-hydrophobic coatings with excellent anti-icing and thermoresponsive deicing performance.* Journal of Materials Chemistry A, 2015. **3**(43): p. 21637-21646.
34. Dhyani, A., et al., *Surface design strategies for mitigating ice and snow accretion.* Matter, 2022. **5**(5): p. 1423-1454.
35. Memon, H., et al., *Durability enhancement of low ice adhesion polymeric coatings.* Progress in Organic Coatings, 2021. **151**: p. 106033.
36. Villeneuve E, Blackburn C, Volat C. Design and development of an experimental setup of electrically powered spinning rotor blades in icing wind tunnel and preliminary testing with surface coatings as hybrid protection solution. Aerospace 2021;8(4):98.

37. Rønneberg S, He J, Zhang Z. The need for standards in low ice adhesion surface research: a critical review. J Adhes Sci Technol 2020;34(3):319–47.
38. Allard T, et al. A Large-Scale Rotor Test Platform for Atmospheric Icing Simulation and Passive Ice Protection Evaluation. Results Eng 2025:108450.
39. Andrews E, Lockington N. The cohesive and adhesive strength of ice. J Mater Sci 1983;18(5):1455–65.
40. Ding L, et al. Experimental Study on Adhesive Characteristics of Aircraft Dynamic Icing. Energies 2023;16(13):5037.
41. Moghadam SG, et al. To be or not to be a hydrophobic matrix? the role of coating hydrophobicity on anti-icing behavior and ions mobility of ionic liquids. Chem Eng J 2024;485:149696.
42. Ma L, et al. An exploratory study on using Slippery-Liquid-Infused-Porous-Surface (SLIPS) for wind turbine icing mitigation. Renew Energy 2020;162:2344–60.
43. Godreau, C.F., Paul; Paquet, Yanick; Krenn, Andreas; Wickman, Helena Technical Report on Ice Detection Guidelines for Wind-Energy Applications. 2021.
44. Kraj AG, Bibeau EL. Phases of icing on wind turbine blades characterized by ice accumulation. Renew Energy 2010;35(5):966–72.
45. Xu Z, et al. A parametric study on the effect of liquid water content and droplet median volume diameter on the ice distribution and anti-icing heat estimation of a wind turbine airfoil. Results Eng 2024;22:102121.
46. Fortin G, Perron J. Spinning rotor blade tests in icing wind tunnel. 1st AIAA Atmos Space Environ Conf 2009.
47. Harvey D, Momen G. Dev a Test Appar Meas Tensile Prop Accreted Ice 2024.
48. Das S, et al. A review on superhydrophobic polymer nanocoatings: recent development and applications. Ind Eng Chem Res 2018;57(8):2727–45.
49. Li X, et al. Formation of icephobic film from POSS-containing fluorosilicone multiblock methacrylate copolymers. Prog Org Coat 2015;89:150–9.
50. Palraj S, et al. Corrosion and wear resistance behavior of nano-silica epoxy composite coatings. Prog Org Coat 2015;81:132–9.

51. Wang X, et al. Mechanical, electrochemical, and durability behavior of graphene nano-platelet loaded epoxy-resin composite coatings. Composites Part B Engineering 2019;176:107103.
52. Yu Y, Rong MZ, Zhang MQ. Friction and wear of epoxy composites containing silica nanoparticles grafted by hyperbranched aromatic polyamide. Polym Polym Compos 2012;20(8):673–82.
53. Liu J, et al. Development and evaluation of poly (dimethylsiloxane) based composite coatings for icephobic applications. Surf Coat Technol 2018;349:980–5.
54. Nistal A, Ruiz-Gonzalez A, Choy K-L. Robust icephobic nanocomposite coatings with superior abrasion resistance. Appl Mater Today 2022;27:101480.
55. Raman A, et al. Electrospun nanofibers as effective superhydrophobic surfaces: a brief review. Surf Interfaces 2021;24:101140.
56. He Z, et al. Room temperature characteristics of polymer-based low ice adhesion surfaces. Sci Rep 2017;7(1):42181.
57. Hejazi V, Sobolev K, Nosonovsky M. From superhydrophobicity to icephobicity: forces and interaction analysis. Sci Rep 2013;3(1):2194.
58. Khammas R, Koivuluoto H. Durable icephobic slippery liquid-infused porous surfaces (SLIPS) using flame-and cold-spraying. Sustainability 2022;14(14):8422.
59. Kim JH, et al. Durable ice-lubricating surfaces based on polydimethylsiloxane embedded silicone oil infused silica aerogel. Appl Surf Sci 2020;512:145728.
60. Laroche A, et al. Silicone nanofilaments grown on aircraft alloys for low ice adhesion. Surf Coat Technol 2021;410:126971.
61. Qin CC, Mulroney AT, Gupta MC. Anti-icing epoxy resin surface modified by spray coating of PTFE Teflon particles for wind turbine blades. Mater Today Commun 2020;22:100770.
62. Tuteja A. Designing durable icephobic surfaces. APS March Meet Abstr 2017.
63. Chen T, et al. Influence of substrate initial temperature on adhesion strength of ice on aluminum alloy. Cold Reg Sci Technol 2018;148:142–7.
64. Rønneberg S, et al. The effect of ice type on ice adhesion. AIP Adv 2019;9(5).
65. Shi W, et al. Icing and adhesive characteristics of iced airfoils under rime ice conditions. Coatings 2025;15(5):606.

3.12 Major Contributions

In this paper, Ghazal Minoofar and Thomas Allard contributed together to the establishment of the methodology leading to the experiments. Ghazal Minoofar worked on the push-off and CAT tests while Thomas Allard led the large-scale experiment. Their work was supervised by Gelareh Momen, Éric Villeneuve, Derek Harvey and Reza Jafari who contributed as well to the manuscript draft. The redaction was carried out by Ghazal Minoofar, Thomas Allard Eric Villeneuve and Derek Harvey, with Thomas Allard taking significant responsibility for the analysis and interpretation of the results.

CHAPTER 4

CONCLUSION

As shown in this research, wind energy production in cold climates remains significantly affected by the problematic of atmospheric icing, which degrades aerodynamic performance, increases mechanical loads, and can lead to extended production downtime. Despite the growing importance of wind energy in northern regions, the understanding of ice adhesion and shedding mechanisms on rotating wind turbine blades remains limited, largely due to the lack of experimental platforms capable of reproducing representative icing conditions at manageable and relevant scales. This context justifies the need for controlled, large-scale experimental tools to bridge the gap between laboratory-scale testing and field observations.

To address this problem, the primary objective of this research was to complete the development of a large-scale rotating-blade test bench dedicated to atmospheric icing studies and to establish a reliable and precise experimental methodology for centrifugal ice adhesion measurements. This work first focused on the comprehensive calibration and characterization of the icing conditions within the cold room by evaluating key governing parameters identified, including air temperature, liquid water content (LWC), median volume diameter (MVD), and precipitation intensity. An optimized test procedure was then developed to quantify ice adhesion on aluminum under centrifugal loading at two target temperatures which produced rime and glaze ice, the main ice types at the source of the icing problems. This procedure included the integration of an ice cohesive strength measurement apparatus to improve accuracy in cases of partial detachment. Finally, the reliability and repeatability of the test bench and procedure were assessed through an extensive experimental campaign conducted on the rotating aluminum blades under conditions relevant to wind turbine icing.

The experimental methodology resulting from the first part of the study relies on the controlled reproduction of critical icing scenarios and on the direct observation of ice fracture mechanisms under dynamic loading. To do so, the ice properties and fracture mechanisms were precisely measured and characterized using high-speed imaging and volumetric numerical scanning and related to the icing conditions. The results demonstrate a high level of stability of the climatic parameters within the icing chamber, ensuring repeatable and controlled test conditions. The accumulated ice shapes were consistent with expected atmospheric ice types, and the fracture modes observed on aluminum blades included mostly mixed failures, presenting cohesive and adhesive shedding, in agreement with mechanisms reported in other similar test benches. The scale of the ice accretions and the measured adhesion values showed good representativity with respect to field conditions. In addition, the dedicated cohesive strength study provided values consistent with published data, while emphasizing the importance of measuring this parameter directly for the specific experimental configuration in order to correctly interpret adhesion results.

In the second part of the study, presented in detail in the second published paper, the precedingly developed methodology was applied to evaluate the performance of different blade surface materials, notably aluminum, a wind turbine gelcoat from the industrial partners, and an icephobic coating. Under controlled icing conditions, the results revealed a significant reduction in ice adhesion for the passive coating compared to the reference substrates. These findings confirm the relevance of passive ice protection solutions and demonstrate the ability of the large-scale test bench to characterize material performance under realistic icing and loading conditions. The adhesion values obtained match the adhesion reduction factors observed for similar passive ice protection solutions on rotating blades of similar substrates.

Although the test platform proved to be highly relevant for the study of wind turbine icing, several improvements could increase its capabilities. A starting point would be the integration of a slip ring which would allow the evaluation of active and hybrid de-icing systems in addition to passive solutions. Additionally, since the experimental procedure separates the icing phase from the shedding phase, implementing icing in rotation at higher rotational speeds would improve the representativity of critical blade tip conditions during severe icing events for wind turbines. Another important improvement would be to increase the number of tests performed for each experimental condition to strengthen the statistical significance of the results. Although this would be challenging due to the complexity of the experimental procedure and the large number of variables involved, it would substantially enhance the robustness of the findings and their relevance for real-world applications. Finally, coupling experimental results with numerical ice fracture simulations would provide deeper insight into detachment mechanisms.

These improvements will widen its potential as an essential tool for atmospheric icing studies and their impact on northern regions wind farms. Accordingly, as this test platform's validation is now complete, following research projects in this facility will continue to build on the basis that was established with this work and push forward the scientific comprehension of atmospheric icing on wind turbines.

Overall, this large-scale experimental platform represents a meaningful step toward more accurate and representative evaluation of icing phenomena and mitigation strategies for wind energy applications. By enabling controlled, repeatable, and realistic testing conditions, this work contributes to the development of more effective ice protection approaches and supports the broader objective of improving the efficiency and reliability of renewable energy systems. In this way, it aligns with the fundamental need to manage energy transfers more intelligently and sustainably in order to limit the environmental impact of human activity.

REFERENCES

1. Lamraoui, F., et al., *Atmospheric icing severity: Quantification and mapping.* Atmospheric Research, 2013. 128: p. 57-75.

2. Fortin, G., *Simulation de l'accrétion de glace sur un obstacle bidimensionnel par la méthode des bissectrices et par la modélisation des ruisselets et des gouttes de surface*. 2003: Université du Québec à Chicoutimi.

3. Caccia, F. and A. Guardone, *Numerical simulations of ice accretion on wind turbine blades: are performance losses due to ice shape or surface roughness?* Wind Energ. Sci., 2023. 8(3): p. 341-362.

4. Fakorede, O., et al., *Ice protection systems for wind turbines in cold climate: characteristics, comparisons and analysis.* Renewable and Sustainable Energy Reviews, 2016. 65: p. 662-675.

5. Palanque, V., et al., *Experimental measurement and expression of atmospheric ice Young's modulus according to its density.* Cold Regions Science and Technology, 2023. 212: p. 103890.

6. Parent, O. and A. Ilinca, *Anti-icing and de-icing techniques for wind turbines: Critical review.* Cold regions science and technology, 2011. 65(1): p. 88-96.

7. Laakso, T., E. Peltola, and B. Tammelin, *Wind turbines in icing environment: Improvement of tools for siting, certification and operation: new icetools.* 2005.

8. Jolin, N., et al., *Wind turbine blade ice accretion: A correlation with nacelle ice accretion.* Cold Regions Science and Technology, 2019. 157: p. 235-241.

9. Hochart, C., et al., *Wind turbine performance under icing conditions.* Wind Energy: An International Journal for Progress and Applications in Wind Power Conversion Technology, 2008. 11(4): p. 319-333.

10. Mayer, C., et al., *Wind tunnel study of electro-thermal de-icing of wind turbine blades.* International Journal of Offshore and Polar Engineering, 2007. 17(03).

11. Shu, L., et al., *Numerical and experimental investigation of threshold de-icing heat flux of wind turbine.* Journal of Wind Engineering and Industrial Aerodynamics, 2018. 174: p. 296-302.

12. Andrews, E. and N. Lockington, *The cohesive and adhesive strength of ice.* Journal of materials science, 1983. 18: p. 1455-1465.

13. Stendardo, L., et al., *Reframing ice adhesion mechanisms on a solid surface.* Applied Surface Science, 2023. 641: p. 158462.

14. Ras, R.H. and A. Marmur, *Non-wettable surfaces: theory, preparation and applications*. 2016: Royal Society of Chemistry.

15. Tarquini, S., et al., *Investigation of ice shedding properties of superhydrophobic coatings on helicopter blades.* Cold Regions Science and Technology, 2014. 100: p. 50-58.

16. Work, A. and Y. Lian, *A critical review of the measurement of ice adhesion to solid substrates.* Progress in Aerospace Sciences, 2018. 98: p. 1-26.

17. Godreau, C., et al., *Definition of Best Practice for Testing Icephobic Surfaces.* 2022.

18. Han, Y., J. Palacios, and S. Schmitz, *Scaled ice accretion experiments on a rotating wind turbine blade.* Journal of Wind Engineering and Industrial Aerodynamics, 2012. 109: p. 55-67.

19. Getz, D. and J. Palacios, *Design Procedures and Experimental Verification of an Electro-Thermal De-Icing System for Wind Turbines.* Wind Energy Science Discussions, 2020. 2020: p. 1-19.

20. Getz, D., *Design, Modeling and Testing of an Electro-Thermal Ice Protection System for Wind Turbines.* 2020.

21. Fortin, G., A. Beisswenger, and J. Perron. *Centrifuge adhesion test to evaluate icephobic coatings*. in *AIAA Atmospheric and Space Environments Conference*. 2010.

22. Fortin, G. and J. Perron. *Spinning rotor blade tests in icing wind tunnel*. in *1st AIAA Atmospheric and Space Environments Conference*. 2009.

23. Li, X., et al., *An Experimental Study on Blade Surface De-Icing Characteristics for Wind Turbines in Rime Ice Condition by Electro-Thermal Heating.* Coatings, 2024. 14(1): p. 94.

24. Villeneuve, E., C. Blackburn, and C. Volat, *Design and development of an experimental setup of electrically powered spinning rotor blades in icing wind tunnel and preliminary testing with surface coatings as hybrid protection solution.* Aerospace, 2021. 8(4): p. 98.